CGRP Signals from Endosomes of Schwann Cells to Elicit Migraine Pain

Francesco De Logu
University of Florence
Romina Nassini
University of Florence
Alan Hegron
College of Dentistry, New York University, New York
Lorenzo Landini
University of Florence https://orcid.org/0000-0002-3933-2497
Dane Jensen
NYU College of Dentistry https://orcid.org/0000-0001-6540-2375
Rocco Latorre
New York University, New York
Julia Ding
Columbia University, New York
Matilde Marini
University of Florence
Daniel Souza Monteiro de Araujo
https://orcid.org/0000-0003-1115-725X
Paulina Ramírez-Garcia
Monash Institute of Pharmaceutical Sciences
Michael Whittaker
Monash University
Jeffri Retamal
Monash Institute of Pharmaceutical Sciences
Mustafa Titiz
University of Florence
Alessandro Innocenti
Careggi University Hospital
Nicholas Veldhuis
Monash Institute of Pharmaceutical Sciences https://orcid.org/0000-0002-8902-9365
Thomas Davis
University of Queensland
Brian Schmidt

New York University https://orcid.org/0000-0002-2409-8984
Nigel Bunnett
Columbia University https://orcid.org/0000-0003-3367-0644
Pierangelo Geppetti (geppetti@unifi.it)
University of Florence https://orcid.org/0000-0003-3797-8371

Article

Keywords: CGRP, CLR, RAMP1, Schwann cell, endosome, ROS, TRPA1, migraine, pain, allodynia

Posted Date: August 24th, 2021

DOI: https://doi.org/10.21203/rs.3.rs-758153/v1

Version of Record: A version of this preprint was published at Nature Communications on February 3rd, 2022. See the published version at https://doi.org/10.1038/s41467-022-28204-z.

Abstract

Efficacy of monoclonal antibodies against calcitonin gene-related peptide (CGRP) or its receptor (calcitonin receptor-like receptor/receptor activity modifying protein-1, CLR/RAMP1) implicates peripherally-released CGRP in migraine pain. However, the site and mechanism of CGRP-evoked migraine pain remain unknown. By cell-selective RAMP1 gene deletion, we reveal that CGRP released from mouse cutaneous trigeminal fibers targets CLR/RAMP1 on surrounding Schwann cells to evoke periorbital mechanical allodynia. CLR/RAMP1 activation in human and mouse Schwann cells generates long-lasting signals from endosomes that evoke cAMP-dependent formation of NO. NO, by gating Schwann cell transient receptor potential ankyrin 1 (TRPA1), releases ROS, which in a feed-forward manner sustain allodynia *via* nociceptor TRPA1. When encapsulated into nanoparticles that release cargo in acidified endosomes, a CLR/RAMP1 antagonist provides superior inhibition of CGRP signaling and allodynia in mice. The CGRP-mediated neuronal/Schwann cell pathway is critical to mediate allodynia associated with neurogenic inflammation, thus contributing to the pro-migraine action of CGRP.

Introduction

For almost a century it has been known that cutaneous tissue injury elicits a local vascular response, referred to as neurogenic inflammation, that is associated to a wider area of increased sensitivity to mechanical stimuli[1]. A subset of C-fiber primary afferents, which mediate neurogenic inflammation, is the main source of the neuropeptides substance P (SP) and calcitonin gene related peptide (CGRP)[2, 3]. In rodents, noxious stimuli such as capsaicin, a pungent agonist of the transient receptor potential vanilloid 1 (TRPV1) channel[4], evoke peripheral release of CGRP which induces arteriolar vasodilatation[2] and of SP which elicits plasma protein extravasation [5], and produce sensory responses, which encompasses acute nociception and prolonged mechanical allodynia[6]. Capsaicin administration to the human skin elicits a similar pattern of responses, consisting of local cutaneous vasodilatation, but not plasma extravasation[7], and focal and transient burning pain (min) associated with widespread, sustained mechanical hypersensitivity (hrs)[8]. While CGRP has been identified as the mediator of neurogenic vasodilatation in rodents[2] and humans[9], the cellular and molecular mechanisms underlying mechanical allodynia associated with neurogenic inflammation are unknown.

The efficacy of small molecule antagonists of CGRP receptor[10] and of monoclonal antibodies to CGRP or its receptor[11] highlights the prominent role of CGRP in migraine pain. The poor penetration of the blood brain barrier by some antagonists[12, 13], and monoclonal antibodies[14] underlines the peripheral origin of CGRP-mediated migraine pain. However, little information exists on the proalgesic action of CGRP in the periphery. In mice, intraplantar injection of CGRP evokes mechanical allodynia[15] and systemic CGRP causes facial grimace[16]. CGRP injection into the periorbital area, while failing to evoke spontaneous nociceptive behavior, produces sustained (~ 4 h) periorbital mechanical allodynia (PMA)[17]. CGRP released from trigeminal peripheral terminals contributes to PMA in mice[18] evoked by systemic

(intraperitoneal) administration of the pro-migraine agent glyceryl trinitrate (GTN)[19]. Facial cutaneous allodynia is a hallmark of migraine pain[20, 21]. However, the anatomical site in the peripheral nervous system and the signaling pathways of CGRP-evoked mechanical hypersensitivity, possibly implicated in migraine pain, are unknown.

The CGRP receptor is a heterodimer of calcitonin receptor-like receptor (CLR), a G protein-coupled receptor (GPCR), and receptor activity-modifying protein 1 (RAMP1), a single transmembrane domain CLR chaperone[22]. These two components coexist in cells that mediate the actions of CGRP, for example vascular myocytes[2]. Satellite glial cells and Schwann cells express CLR/RAMP1 and are closely associated with peptidergic sensory neurons[23]. While the extracellular space between the soma of trigeminal neurons and satellite glial cells is not a recognized locus for neurotransmission, the varicosities of C-fibers and the ensheathing Schwann cells are sites where neuropeptides, including CGRP[24], are normally released. Schwann cells from rat sciatic nerve respond to CGRP by increasing intracellular cAMP levels[25] and CLR/RAMP1 are expressed by Schwann cells that wrap CGRP + ve terminals of rat nociceptors[23, 26, 27]. Schwann cells mediate mechanical allodynia in mouse models of neuropathic and cancer pain[28, 29]. Cutaneous Schwann cells can also directly activate sensory nerves to promote mechanical nociception[30]. Although GPCRs are usually considered to signal principally from the plasma membrane, GPCR kinases and β-arrestins (βARRs) rapidly terminate this signaling. Persistent endosomal signaling of GPCRs, including CLR/RAMP1, underlies sustained neuronal activation and nociception in the central nervous system (CNS)[31, 32, 33].

Herein, we hypothesized that mechanical allodynia associated with neurogenic inflammation is mediated by CGRP which targets CLR/RAMP1 in Schwann cells ensheathing peripheral endings of nociceptors. By selective RAMP1 gene deletion in Schwann cells, we reveal that CGRP released from trigeminal terminals causes PMA by paracrine signaling to the surrounding Schwann cells. We also hypothesized that persistent CGRP/CLR/RAMP1 signaling from endosomes in Schwann cells underlies sustained PMA. By using inhibitors of clathrin- and dynamin-mediated endocytosis and stimulus-responsive nanoparticles designed to release CLR/RAMP1 antagonists in acidified endosomes, we found that CLR/RAMP1 endosomal signaling results in a cAMP-dependent release of nitric oxide (NO), which activates transient receptor potential ankyrin 1 (TRPA1), a proalgesic channel and sensor of oxidative stress[34]. TRPA1, *via* NADPH oxidase 1 (NOX1), elicits an oxidative stress-dependent feed-forward mechanism that sustains allodynia. In two recognized mouse models of migraine, induced by systemic CGRP[16] and GTN[18] administration, selective deletion of Schwann cell RAMP1 attenuated PMA.

Results

CGRP evokes PMA by activating Schwann cell CLR/RAMP1

We detected CLR and RAMP1 mRNA and immunoreactivity in primary cultures of human and mouse Schwann cells (HSCs, MSCs) (Fig. 1a, Supplementary Fig. 1a). The S100 + ve mouse Schwann cell line

(IMS32) recapitulated features of primary MSCs, including expression of CLR and RAMP1 mRNA and immunoreactivity (Supplementary Fig. 1a,b) and responsiveness to allyl isothiocyanate, which evoked a TRPA1-dependent increase in Ca^{2+} response (Supplementary Fig. 1c). Immunoreactive CLR and RAMP1 were also detected in S100 + ve Schwann cells in nerve bundles in biopsies of human abdominal and mouse periorbital skin (Fig. 1b).

To assess the role of Schwann cell CLR/RAMP1 in CGRP-evoked PMA, Schwann cell-specific Cre mice (*Plp-Cre*^{ERT}) were crossed with RAMP1 floxed mice *(Ramp1*$^{fl/fl}$) to generate *Plp-Cre*$^{ERT+}$;*Ramp1*$^{fl/fl}$ and *Plp-Cre*$^{ERT-}$;*Ramp1*$^{fl/fl}$ (Control) mice. Unless otherwise specified, all drugs were administered by subcutaneous periorbital injection (Supplementary Table 1). For selective deletion of RAMP1 in Schwann cells of the periorbital region, 4-hydroxytamoxifen (4-OHT) was administered daily for 3 days to *Plp-Cre*$^{ERT+}$;*Ramp1*$^{fl/fl}$ and Control mice. In Control mice CGRP elicited allodynia in the periorbital area (Fig. 1c), but not at a distant site, such as the hind paw (Supplementary Fig. 1d). CGRP-evoked PMA was markedly attenuated in *Plp-Cre*$^{ERT+}$;*Ramp1*$^{fl/fl}$ mice treated with 4-OHT (Fig. 1c). 4-OHT treatment down-regulated RAMP1 immunoreactivity in S100 + ve cells surrounding trigeminal but not sciatic nerve fibers (Fig. 1d) and did not prevent paw mechanical allodynia evoked by intraplantar CGRP (Supplementary Fig. 1e). Intravenous CGRP provokes delayed migraine-like attacks in patients[35]. To mimic the human provocation test, intraperitoneal CGRP was given to Control mice which elicited PMA and paw allodynia (Fig. 1e,f). PMA, but not paw allodynia, was reduced in *Plp-Cre*$^{ERT+}$;*Ramp1*$^{fl/fl}$ mice treated with 4-OHT (Fig. 1e,f). Systemic (intraperitoneal) 4-OHT reduced both PMA and paw allodynia (Supplementary Fig. 1f,g). These results reveal an essential role for CLR/RAMP1 of Schwann cells surrounding periorbital trigeminal endings in sustained PMA elicited by both local and systemic CGRP.

Stimulation of peptidergic trigeminal neurons evokes PMA by activating Schwann cell CLR/RAMP1

To explore the ability of endogenous CGRP to elicit PMA, we administered capsaicin, which activates TRPV1[4] and in rodents stimulates release of both CGRP and SP from terminals of peptidergic nociceptors[3]. Periorbital capsaicin dose-dependently elicited acute (~ 10 min) nociceptive behavior (Fig. 2a) and, like CGRP, caused prolonged (~ 4 h) PMA (Fig. 2b). The proalgesic action was detected in the periorbital area but not in the hind paw (Supplementary Fig. 2a), indicating a local action. TRPV1 deletion (*Trpv1*$^{-/-}$ mice) (Fig. 2c,d) or pretreatment with the TRPV1 antagonist capsazepine (Fig. 2e,f), prevented acute nociception and PMA. An antagonist (L-733,060) of the SP neurokinin 1 (NK_1) receptor, which prevented SP-evoked PMA (Fig. 2g), failed to diminish capsaicin-evoked acute nociception and PMA (Fig. 2h, Supplementary Fig. 2b). Local pretreatment with the histamine H_1 receptor antagonist, astemizole, inhibited SP-evoked PMA (Supplementary Fig. 2c) but did not affect CGRP- or capsaicin-evoked PMA (Supplementary Fig. 2d,e). Pretreatment with the CLR/RAMP1 antagonists, CGRP8-37 or olcegepant, prevented PMA (Fig. 2i,j) but not acute nociception evoked by capsaicin (Supplementary Fig. 2b). Importantly, 4-OHT markedly inhibited capsaicin-evoked PMA (Fig. 2k) but not acute nociception (Supplementary Fig. 2f) in *Plp-Cre*$^{ERT+}$;*Ramp1*$^{fl/fl}$ mice as compared to Control mice. PMA elicited by CGRP or acute nociception and PMA elicited by capsaicin were similar in mice with selective deletion of

RAMP1 in nociceptors (*Adv-Cre*$^{+}$;*Ramp1*$^{fl/fl}$) and Control mice (Fig. 2l,m). In addition, both PMA and paw allodynia were similar in *Adv-Cre*$^{+}$;*Ramp1*$^{fl/fl}$ and Control mice after intraperitoneal CGRP (Fig. 2n,o). Results imply two conclusions. First, CGRP but not SP mediates allodynia resulting from excitation of TRPV1 + ve peptidergic nociceptors. Second, PMA evoked by both endogenous and exogenous CGRP is dependent on CLR/RAMP1 of Schwann cells surrounding peripheral terminals of nociceptors, while the receptor of sensory nerve fibers is not implicated.

Schwann cell CLR/RAMP1 mediates the CGRP-dependent PMA evoked by GTN

Systemic GTN administration provokes migraine-like pain in humans[19]. In mice intraperitoneal GTN elicits PMA[18], that is in part mediated by CGRP release from periorbital trigeminal terminals[18]. Here, we show that systemic (intraperitoneal) GTN elicited PMA (Fig. 3a) and paw allodynia (Fig. 3b) that were similar in Control and *Adv-Cre*$^{+}$;*Ramp1*$^{fl/fl}$ mice. Olcegepant transiently and partially inhibited PMA (Fig. 3a), while did not affect paw allodynia (Fig. 3b) evoked by intraperitoneal GTN in both mouse strains. Deletion of RAMP1 by 4-OHT in *Plp-Cre*$^{ERT+}$;*Ramp1*$^{fl/fl}$ mice partially inhibited PMA (Fig. 3c), but not paw allodynia (Fig. 3d). Importantly, treatment with olcegepant reduced GTN-evoked PMA in Control mice, but failed to further inhibit the response in *Plp-Cre*$^{ERT+}$;*Ramp1*$^{fl/fl}$ mice (Fig. 3c). Paw allodynia was unchanged by olcegepant (Fig. 3d). Together, the findings suggest that Schwann cell CLR/RAMP1 mediates the CGRP-dependent component of PMA in an established mouse model of migraine pain.

Clathrin- and dynamin-mediated endocytosis of CLR/RAMP1 in Schwann cells mediates PMA

We investigated the CLR/RAMP1 signaling pathway in Schwann cells that mediates CGRP-evoked PMA. CGRP-stimulated cAMP formation was measured in HSCs using a virally-encoded cAMP cADDis reporter. CGRP stimulated a prompt concentration-dependent increase in cAMP formation in HSCs that was sustained for > 300 s (Fig. 4a,b; Video S1). The CLR/RAMP1 antagonist olcegepant caused a concentration-dependent inhibition of CGRP-stimulated cAMP formation (Fig. 4c-e).

Endosomal signaling of GPCRs, including CLR/RAMP1, controls nociception[31, 32, 33]. To assess CLR/RAMP1 endocytosis in Schwann cells, we incubated HSCs expressing the early endosome marker Rab5a-GFP with TAMRA-CGRP. In vehicle-treated cells, live cell imaging revealed uptake of TAMRA-CGRP into Rab5a-GFP + ve early endosomes within 10 min that continued for 30 min (Fig. 4f, Video S2). Inhibitors of clathrin (PitStop2, PS2) or dynamin (Dyngo4a, Dy4) prevented the translocation of TAMRA-CGRP to endosomes causing retention of weak TAMRA-CGRP fluorescence at the cell surface (Fig. 4e,f; Video S3,S4). Quantification of TAMRA-CGRP fluorescence intensity in Rab5a-GFP + ve endosomes or the proportion of endosomes containing TAMRA-CGRP confirmed that PS2 and Dy4 inhibited endocytosis of TAMRA-CGRP (Fig. 4g,h). Inactive analogs had no effect. Hypertonic sucrose (0.45 M) inhibits clathrin-mediated endocytosis, including agonist-stimulated endocytosis of GPCRs[36]. Hypertonic sucrose also inhibited the uptake of TAMRA-CGRP in HSCs (Fig. 4g,h, Video S5). Periorbital injection of PS2 or Dy4 prevented CGRP- and capsaicin-evoked PMA, whereas inactive analogs had no effect (Fig. 4i-l). Thus,

CGRP stimulates clathrin- and dynamin-mediated endocytosis of CLR/RAMP1 in Schwann cells, which sustains CGRP-evoked PMA.

CLR activates $G\alpha_s$, $G\alpha_q$ and $G\alpha_i$ and recruits βARR2 to the plasma membrane and endosomes

GPCRs, including CLR/RAMP1, can signal from endosomes by $G\alpha_s$, $G\alpha_q$ and βARR-mediated mechanisms[31, 32, 33]. We used enhanced bystander bioluminescence resonance energy transfer (EbBRET) to study the activation of Gα and recruitment of βARR to the plasma membrane and early endosomes of HEK293T cells expressing human (h) CLR and RAMP1 (HEK-hCLR/RAMP1). CGRP-dependent activation of $G\alpha_s$, $G\alpha_{sq}$ and $G\alpha_{si}$ was assessed using an EbBRET assay that detects recruitment of mini (m) Gα coupled to *Renilla* (R)luc8 to the plasma membrane marker CAAX coupled to RGFP or the early endosome marker Rab5a coupled to tandem (td)RGFP. mGα proteins are N-terminally truncated Gα proteins that freely diffuse throughout the cytoplasm and bind to active conformations of GPCRs. Their translocation to GPCRs reflects Gα activation. $mG\alpha_{sq}$ and $mG\alpha_{si}$ were developed by mutating $mG\alpha_s$ residues to equivalent $G\alpha_q$ and $G\alpha_i$ residues. Recruitment of βARR was assessed by measuring EbBRET between Rluc2-βARR2 and RGFP-CAAX or tdRGFP-Rab5a. CGRP induced a rapid increase in EbBRET between Rluc8-$mG\alpha_s$, Rluc8-$mG\alpha_{sq}$, Rluc8-$mG\alpha_{si}$ and Rluc2-βARR2 with RGFP-CAAX, which was maximal at ~ 300 s and declined over 1000 s (Fig. 5a,b). CGRP increased EbBRET between Rluc8-$mG\alpha_s$, Rluc8-$mG\alpha_{sq}$, Rluc8-$mG\alpha_{si}$ and Rluc2-βARR2 with tdRGFP-Rab5a that was fully sustained for 1300 s (Fig. 5c,d). EbBRET was similarly used to study the activation of Gα and recruitment of βARR2 to the plasma membrane and endosomes of HSCs transfected with hCLR/RAMP1 (CLR/RAMP1 overexpression was required to amplify BRET signals). In HSCs, CGRP increased EbBRET between Rluc8-$mG\alpha_s$, Rluc8-$mG\alpha_{sq}$, Rluc8-$mG\alpha_{si}$ and Rluc2-βARR2 with RGFP-CAAX and tdRGFP-Rab5a (Fig. 5e-h). EbBRET signals were sustained for 1300 s.

To investigate the contribution of endocytosis to the activation of Gα proteins and βARRs in endosomes, we preincubated cells with hypertonic sucrose. CGRP increased EbBRET between hCLR-Rluc8 and tdRGFP-Rab5a in HEK-hCLR/RAMP1 cells, consistent with CLR endocytosis (Fig. 5i). Hypertonic sucrose inhibited these changes, which indicates an inhibition of endocytosis (Fig. 5i). Hypertonic sucrose caused a delayed yet more sustained activation of Rluc8-$mG\alpha_s$, Rluc8-$mG\alpha_{sq}$, Rluc8-$mG\alpha_{si}$ and Rluc2-βARR2 at the plasma membrane (Supplementary Fig. 3a-f), and an almost complete inhibition of activation of Rluc8-$mG\alpha_s$, Rluc8-$mG\alpha_{sq}$, Rluc8-$mG\alpha_{si}$ and Rluc2-βARR2 in endosomes (Fig. 5j,k). Sucrose similarly delayed CGRP-induced recruitment of Rluc8-$mG\alpha_s$, Rluc8-$mG\alpha_{sq}$, Rluc8-$mG\alpha_{si}$ and Rluc2-βARR2 to the plasma membrane (Supplementary Fig. 3g-l) and almost completely inhibited activation of $G\alpha_{s,sq,si}$ and βARR2 in endosomes of HSCs expressing hCLR/RAMP1 (Fig. 5l,m).

To examine the contribution of endosomal CLR/RAMP1 signaling to CGRP-induced cAMP formation, we preincubated HSCs expressing the cADDis cAMP reporter with sucrose or vehicle. In vehicle-treated cells, CGRP stimulated a rapid (1 min) increase in cAMP formation that was sustained for 30 min (Fig. 5n,o). Sucrose reduced but did not abolish the initial response, yet strongly inhibited the sustained phase of

CGRP-stimulated cAMP formation (Fig. 5n,o). Thus, CGRP initially activates Gα and βARR at the plasma membrane, which is followed by sustained activation of Gα and βARR in early endosomes. Endocytosis is necessary for the recruitment of Gα and βARR to endosomes. $G\alpha_s$ continues to signal in endosomes, leading to sustained cAMP formation.

CLR/RAMP1 activation in Schwann cells releases NO, which initiates but does not sustain PMA

We investigated the mechanisms that sustain PMA following CLR/RAMP1 activation and endocytosis in Schwann cells. Pretreatment with CLR/RAMP1 antagonists, olcegepant or CGRP8-37, attenuated PMA evoked by capsaicin and in accordance with previous studies[17, 18] PMA evoked by CGRP (Supplementary Fig. 4a,b). In contrast, antagonists had no effect when administered 60 min after CGRP or capsaicin (Supplementary Fig. 4c-f). Similarly, inhibitors of clathrin- and dynamin-mediated endocytosis had no effect when administered 60 min after CGRP or capsaicin (Supplementary Fig. 4g-j). Thus, once induced by CGRP, CLR/RAMP1 antagonists or inhibitors of CRL/RAMP1 internalization are unable to attenuate PMA. Pre- but not post-treatment with the protein kinase A (PKA) inhibitor, H89, reduced PMA by CGRP and capsaicin (Supplementary Fig. 4k-n). NO has been implicated in CGRP-mediated vascular responses[2]. Although NO can release CGRP with proalgesic functions, the contribution of NO to CGRP-evoked allodynia is uncertain. Pretreatment with an NO synthase (NOS) inhibitor (L-NAME) or an NO scavenger (cPTIO) (Fig. 6a), abrogated CGRP-evoked PMA (Fig. 6b,c). L-NAME and cPTIO pretreatment also attenuated capsaicin-evoked PMA (Fig. 6d,e). However, L-NAME and cPTIO did not affect PMA when administered 60 min after CGRP (Supplementary Fig. 4o,p) or capsaicin (Supplementary Fig. 4q,r). Thus, PKA-dependent NO release[37] evoked by CGRP is necessary to initiate, but is not sufficient to sustain, allodynia.

In vitro findings recapitulated *in vivo* results. HSCs, MSCs and IMS32 cells predominantly expressed NOS3 (eNOS) mRNA, with little or no expression of NOS1 and NOS2 (nNOS and iNOS, respectively) mRNA (Fig. 6f,g; Supplementary Fig. 4s). In both HSCs and IMS32 cells, CGRP elicited a transient increase in NOS3 phosphorylation (*i.e.*, activation), consistent with NO generation, which peaked at 5–10 min and declined within 30–60 min (Fig. 6h). In HSCs and IMS32 cells, the cAMP increase elicited by CGRP was prevented by olcegepant, CGRP8-37 and an adenylyl cyclase inhibitor (SQ22536), but not by L-NAME (Fig. 6i). The increase in cAMP evoked by CGRP but not that elicited by forskolin was reduced in cultured MSCs obtained from *Plp-Cre*$^{ERT+}$;*Ramp1*$^{fl/fl}$ mice as compared to Control mice treated with intraperitoneal 4-OHT (Fig. 6j). In contrast, the CGRP-evoked increase in NO was attenuated by all these interventions, including NOS inhibition (Fig. 6k). The cAMP increase evoked by forskolin was unaffected by CLR/RAMP1 antagonism and NOS inhibition, and olcegepant failed to inhibit NO release by the NO donor NONOate (Supplementary Fig. 4t,u), indicating selectivity. PS2 and Dy4, but not their inactive analogs, inhibited CGRP-mediated NO release but did not affect NONOate-stimulated NO release (Supplementary Fig. 4v), further supporting selectivity. These results suggest that clathrin- and dynamin-dependent endocytosis and endosomal CLR/RAMP1 signaling evoke NOS activation and NO generation in Schwann cells.

Schwann cell TRPA1 mediates CGRP-evoked PMA

NO belongs to a series of reactive oxygen species (ROS) that target TRPA1[38]. TRPA1 is coexpressed with TRPV1 and CGRP in a subpopulation of primary sensory neurons[39]. TRPA1 is expressed in Schwann cells of nerve bundles of human skin and mouse sciatic nerve, where it mediates mechanical allodynia in rodent models of pain[28, 40]. Immunoreactive TRPA1 was coexpressed with RAMP1 in S100+ve Schwann cells in human abdominal and mouse periorbital cutaneous nerves bundles (Fig. 7a). Thus, CLR/RAMP1 might engage signaling pathways that activate TRPA1 in trigeminal Schwann cells to initiate allodynia (Fig. 7b). The hypothesis that CLR/RAMP1 activates TRPA1 to induce allodynia was supported by the observation that both CGRP- and capsaicin-evoked PMA were reduced in *Trpa1*$^{-/-}$ mice and in mice with sensory neuron-specific deletion of TRPA1 (*Adv-Cre*$^{+}$*;Trpa1*$^{fl/fl}$) (Fig. 7c,d).

We next investigated the signaling pathway by which the CLR/RAMP1 activates TRPA1. In HSCs and IMS32 cells, CGRP stimulated a slowly developing yet sustained increase in Ca^{2+} response and increased H_2O_2 levels (Fig. 7e-g). Olcegepant, CGRP8-37, SQ22536, H89, L-NAME, Ca^{2+}-free medium, ROS scavenger (PBN) or a NOX1 inhibitor (ML171) attenuated these responses (Fig. 7e-g). A TRPA1 antagonist (A967079) inhibited CGRP-stimulated Ca^{2+} and H_2O_2 responses (Fig. 7e-g) but did not affect CGRP-stimulated NO formation (Fig. 7h). CGRP-evoked Ca^{2+} responses were reduced in Schwann cells from *Trpa1*$^{-/-}$ mice (Supplementary Fig. 5a). These results support the hypothesis that CGRP liberates NO, which activates Schwann cell TRPA1; activated TRPA1 promotes a Ca^{2+}-dependent H_2O_2 generation that sustains a feed-forward mechanism comprising TRPA1 channel engagement and ROS release.

In vivo results support the existence of a CGRP-evoked proalgesic pathway that is initiated by an NO-dependent mechanism and sustained by ROS-mediated TRPA1 engagement. Whereas CLR/RAMP1 antagonists or NO inhibitors attenuated PMA only if given before CGRP or capsaicin, both pre- and post-treatment with a TRPA1 antagonist, a ROS scavenger and a NOX1 inhibitor reduced PMA (Fig. 7i-k; Supplementary Fig. 5b-d). Although pretreatment with TRPA1 or ROS inhibitors did not affect the acute nociception, they inhibited capsaicin-evoked PMA (Supplementary Fig. 5b-d). Post-treatment also attenuated capsaicin-evoked PMA (Supplementary Fig. 5b-d). These findings highlight the mechanistic differences between acute nociception and delayed PMA. After an initial and transient NO-dependent phase, PMA is sustained by persistent ROS liberation, which targets TRPA1 in Schwann cells. This hypothesis is robustly supported by the observation that PMA evoked by CGRP or capsaicin was markedly attenuated in mice with selective deletion of TRPA1 in Schwann cells (*Plp-Cre*$^{ERT+}$*;Trpa1*$^{fl/fl}$) (Fig. 7l).

Targeting endosomal CGRP signaling provides superior relief of CGRP- and capsaicin-evoked PMA

The finding that persistent GPCR signaling from endosomes mediates pain transmission suggests that GPCRs in endosomes rather than at the plasma membrane are a valid and perhaps superior target for the treatment of pain[31, 32, 33]. Nanoparticles have been used to deliver chemotherapeutics to tumor,

where endocytosis and endosomal escape are necessary for drug delivery to cytosolic and nuclear targets[41]. The realization that GPCRs within endosomes are a therapeutic target, raises the possibility of exploiting the acid microenvironment of endosomes as a stimulus for nanoparticle disassembly and release of antagonist cargo[32].

To target CLR in endosomes, we generated self-assembling soft polymer nanoparticles containing a CLR antagonist. Diblock copolymers were synthesized with a hydrophilic shell of P(PEGMA-co-DMAEMA) and a hydrophobic core of P(DIPMA-co-DEGMA) (Fig. 8a). Gel permeation chromatography and ^{1}H-nuclear magnetic resonance (^{1}H-NMR) confirmed the molecular weight and composition of nanoparticles (Supplementary Fig. 6a-d). Nanoparticles were self-assembled with MK-3207, a potent hydrophobic antagonist of human CLR/RAMP1, forming DIPMA-MK-3207 (Fig. 8a). Empty nanoparticles (DIPMA-Ø) were used as a control. Nanoparticles were uniformly spherical, with similar diameter (30-35 nm) and ζ-potential (-0.4-1.3 mV) (Fig. 8b,c). DIPMA nanoparticles demonstrate a pH-dependent cargo release at pH<~6.5, consistent with the protonation of the DIPMA tertiary amine (pK_a 6.1), charge repulsion and disassembly[32]. DIPMA nanoparticles enter cells by clathrin- and dynamin-mediated endocytosis and disassemble in acidic early endosomes[32]. To determine whether DIPMA nanoparticles target endosomes containing CLR/RAMP1, HSCs expressing early endosomal antigen-1-GFP (EEA1-GFP) were incubated with DIPMA-Cy5 for 30 min to allow accumulation in EEA1-GFP+ve endosomes (Fig. 7d, Video S6). Cells were then incubated with TAMRA-CGRP, which was detected in endosomes containing Cy5-DIPMA within 5-10 min (Fig. 8d, Video S6). Thus, DIPMA nanoparticles accumulate with CLR/RAMP1 in early endosomes of Schwann cells.

To determine whether DIPMA-MK-3207 can antagonize CLR in endosomes, we measured CGRP-stimulated cAMP formation using the CAMYEL cAMP BRET sensor, which detects total cellular cAMP. HEK293 cells expressing rat CLR/RAMP1 (HEK-rCRL/RAMP1) were preincubated with graded concentrations of DIPMA-MK-3207 or free MK-3207, DIPMA-Ø or vehicle (control) for 30 min. Beginning at 0 min, baseline BRET was measured for 5 min, and cells were then challenged with CGRP. At 10 min, cells were washed to remove extracellular CGRP, and BRET was measured up to 35 min. In vehicle-treated cells, CGRP stimulated a prompt increase in cAMP formation (1st phase, 6-10 min) that gradually declined after agonist removal from the extracellular fluid (2nd phase, 11-35 min) (Fig. 8e). DIPMA-Ø did not affect this response. Free MK-3207 and DIPMA-MK-3207 (100, 316 nM) both inhibited CGRP-evoked cAMP in the 1st phase to a similar extent (Fig. 8f). During the 2nd phase, free MK-3207 was inactive at all concentrations whereas DIPMA-MK3207 (31.6, 100, 316 nM) strongly inhibited responses (Fig. 8g). The results suggest that DIPMA-MK3207 can antagonize the sustained phase of CGRP-stimulated formation of cAMP, which is attributable to endosomal CLR/RAMP1 signaling.

To assess antagonism of the pain signaling pathway in HSCs, we measured CGRP-evoked changes in Ca^{2+} response, which depend on endosomal CGRP signaling and activation of TRPA1. HSCs were preincubated with graded concentrations of DIPMA-MK-3207 or MK-3207 for 20 min to allow accumulation in endosomes, and washed to remove extracellular compounds. At 10 min after washing,

cells were challenged with CGRP and Ca^{2+} response was measured as an index of TRPA1 activity. DIPMA-MK-3207 inhibited CGRP-evoked increase in Ca^{2+} response (IC_{50} 15.4 nM, 95% confidence interval, 10.9 - 21.0 nM) more potently than free MK-3207 (IC_{50} 2.9 µM, 95% confidence interval, 1.9 - 4.2 µM, P<0.0001) (Fig. 8h). To assess antinociception, DIPMA-MK-3207 or free MK-3207 (0.1, 0.3, 1.0 pmol) was injected into the periorbital region 30 min before periorbital injection of CGRP or capsaicin. DIPMA-MK-3207 (0.3, 1.0 pmol) more effectively inhibited PMA than the same doses of free MK-3207 (Fig. 8i). DIPMA-Ø had no effect. Thus, endosomal targeting enhances the efficacy of a CLR/RAMP1 antagonist in a preclinical model of migraine pain.

Discussion

The major findings of the present study, supported by genetic and pharmacological evidence, are that CGRP causes migraine pain by activating CLR/RAMP1 of Schwann cells, CLR/RAMP1 signal from endosomes of Schwann cells to activate pain pathways, and endosomal CLR/RAMP1 can be targeted using nanoparticles and endocytosis inhibitors to relieve CGRP-evoked migraine pain. CLR/RAMP1 activation and trafficking to endosomes results in a persistent cAMP-dependent activation of NOS and generation of NO, a mediator of migraine pain[19]. The role of NO in PMA is crucial, yet transient, as it is temporally limited to the engagement of TRPA1/NOX1, which releases ROS with a dual function. On one hand, ROS target TRPA1/NOX1 of Schwann cells to maintain ROS generation by a feed-forward mechanism. On the other hand, as suggested by experiments with selective TRPA1 deletion in primary sensory neurons, ROS target TRPA1 on nociceptors to signal allodynia to the CNS.

Periorbital capsaicin injection elicited acute nociception mediated by TRPV1 excitation and ensuing afferent discharge, which signals pain to the CNS. In a larger cutaneous area, capsaicin evoked delayed and prolonged PMA. While the acute pain response is most likely dependent on ion influx associated with TRPV1 activation, the mechanism underlying mechanical hypersensitivity[8, 42] has remained elusive. Our findings support the existence of a paracrine mechanism that underlies PMA associated with neurogenic inflammation. We suggest that capsaicin locally activates TRPV1 + ve nerve fibers to generate action potentials that propagate antidromically into collateral fibers which release CGRP in a broader area, thus eliciting widespread PMA. PMA depends on the interaction between peptidergic nerve fibers, surrounding Schwann cells and nociceptive neurons that convey allodynic signals to the CNS. CGRP liberated from the varicosities of trigeminal TRPV1 + ve nerve fibers binds to CLR/RAMP1 of adjacent Schwann cells.

CGRP released from peptidergic C-fibers has been hypothesized to target CLR/RAMP1 on adjacent non-peptidergic Aδ-fibers[43] within the node of Ranvier[26] to mediate migraine pain. Present results in mice with selective RAMP1 deletion in primary sensory neurons firmly support the view that nociceptors are not the target of CGRP to evoke PMA, which, instead, implicates the role of Schwann cells that wrap their terminals. A limitation of the present study is that we cannot distinguish between TRPV1-expressing nerve fibers that release CGRP and TRPA1-expressing nerve fibers that are targeted by Schwann cell ROS and convey allodynic signals centrally. Indeed, TRPV1 and TRPA1 may coexist in the same population of

CGRP-expressing Aδ- or C-fiber primary sensory neurons[2,39]. Most Schwann cells in Remak bundles contain multiple unmyelinated axons belonging to morphologically and functionally different neurons, including CGRP + ve and isolectin B4 + ve fibers[44]. Moreover, the bulk of CGRP is expressed in C-fiber nociceptors[2]. Thus, we cannot discriminate between the three possibilities that ROS from Schwann cells target TRPA1 on the same Aδ- or C-fiber that releases CGRP, on a different C-fiber of the same Remak bundle, or on a different adjacent Aδ-fiber. The observation that both C-fiber and Aδ-fiber nociceptors contribute to capsaicin-evoked hypersensitivity in humans[45] supports the hypothesis that both types of neurons[26, 43] are implicated in CGRP-mediated allodynia.

CLR/RAMP1 signals from endosomes by G-protein-mediated mechanisms that activate a subset of compartmentalized signals, including cytosolic protein kinase C and nuclear extracellular signal regulated kinase; these kinases regulate excitation of spinal neurons and pain transmission[33]. Our results show that CLR/RAMP1 activates $G\alpha_s$, $G\alpha_q$ and $G\alpha_i$ and recruits βARRs in endosomes of Schwann cells, determined by EbBRET. Inhibitors of clathrin- and dynamin-mediated endocytosis blocked the recruitment of CLR/RAMP1, Gα and βARR to endosomes, which presumably requires CLR/RAMP1 endocytosis. GPCR/Gα signaling complexes have also been detected in endosomes by using conformationally selective nanobodies[46]. The observation that endocytosis inhibitors attenuated CGRP-stimulated formation of cAMP and activation of NOS and TRPA1 reveals a central role for CLR/RAMP1 signaling in endosomes of Schwann cells in CGRP-evoked periorbital pain. Endocytosis of other Gs-coupled GPCRs is also necessary for the full repertoire of cAMP-mediated signaling outcomes, which entails endosomal recruitment of adenylyl cyclase 9[47] and assembly of metastable accumulations of PKA[48]. We found that a nanoparticle-encapsulated CLR/RAMP1 antagonist, which targeted CLR/RAMP1 in endosomes and released cargo in the acidified endosomal microenvironment[32], also attenuated CGRP-stimulated cAMP formation and blunted TRPA1 activation.

The observation that periorbital injection of inhibitors of clathrin and dynamin and of DIPMA-MK-3207 prevented CGRP- and capsaicin-evoked PMA provides the first evidence for a prominent role of endosomal CGRP signaling of pain from a peripheral site. The finding that nanoparticle encapsulation enhanced the potency of a CGRP antagonist for inhibition of endosomal signaling and resultant nociception supports the hypothesis that CLR/RAMP1 in endosomes is a target for migraine pain. Nanoparticle encapsulation similarly boosts the efficacy of an NK_1 receptor antagonist in preclinical models of inflammatory and neuropathic pain[32]. An antagonist of CLR/RAMP1 conjugated to a membrane lipid cholestanol also accumulates in endosomes and provides superior relief from pain[33], which reinforces the importance of CLR/RAMP1 endosomal signaling for pain transmission.

Limitations of the present study include uncertainty about the nature of the CLR/RAMP1 signaling complex in endosomes of Schwann cells, which warrants further investigation by proteomics approaches. Although some of the pharmacological inhibitors used to dissect the signaling pathway can have non-specific actions, we bolstered confidence in selectivity by using inhibitors of the same pathway and by genetic deletion of GPCRs and TRP channels. Our findings reveal a prominent role for

CLR/RAMP1 in Schwann cells for CGRP-evoked periorbital pain. Future studies will investigate the role of this pathway in preclinical models of migraine pain.

Monoclonal antibodies to CGRP, although beneficial, are not effective in all patients[11]. While non-CGRP-dependent mechanisms might explain this failure[49], CGRP or CLR/RAMP1 antibodies likely do not inhibit CGRP signaling in endosomes. The small molecule CLR/RAMP1 antagonist, rimegepant, was found to resolve migraine attacks in patients treated with the anti-CLR/RAMP1 monoclonal antibody, erenumab[50]. This unexpected result was interpreted by the inherent membrane permeability of the lipophilic antagonist rimegepant[51] that might favor inhibition of CGRP signaling in endosomes[50], while neither receptor-targeted nor ligand-targeted monoclonal antibodies internalized with CLR/RAMP1 activated by CGRP[52]. Our results showing a superior inhibition of CGRP signaling in Schwann cells and of PMA by DIPMA-MK-3207, which selectively targets receptor activity in endosomes, reveals a better approach to control migraine pain. By inhibiting CLR/RAMP1 translocation to endosomes, inhibitors of clathrin- and dynamin-mediated endocytosis might offer an alternate therapeutic approach for migraine pain.

In 1936, Sir Thomas Lewis postulated[1] that in human skin action potentials are carried antidromically from the injured nerve terminal to collateral branches from where a chemical substance is released that produces the flare and increases the sensitivity of other fibers responsible for pain. CGRP has been previously identified as the mediator responsible for neurogenic vasodilatation in rodents[2], and in humans[9]. Herein, we propose that CGRP is the 'chemical substance' that, *via* the essential role of endosomal CLR/RAMP1, TRPA1/NOX1 and oxidative stress of surrounding Schwann cells, sustains the enhanced sensitivity of primary sensory neurons associated with neurogenic inflammation (Fig. 9). Results obtained in the two mouse models of migraine evoked by systemic CGRP or GTN suggest that the proalgesic pathway activated by CGRP in Schwann cells is implicated in migraine pain and is the target of peripherally acting anti-CGRP medicines.

Methods

Experimental model and subject details

Animals. Male mice were use throughout (25–30 g, 5–8 weeks). The following strains of mice were used C57BL/6J mice (Charles River, RRID:IMSR_JAX:000664); wild-type (*Trpa1*$^{+/+}$) and TRPA1-deficient (*Trpa1*$^{-/-}$; B6129P-Trpa1^{tm1Kykw}/J; RRID:IMSR_JAX:006401, Jackson Laboratory) mice[53]; wild-type (*Trpv1*$^{+/+}$) and TRPV1-deficient (*Trpv1*$^{-/-}$; B6129X1-Trpv1^{tm1Jul}/J, RRID:IMSR_JAX:003770, Jackson Laboratory) mice. Genetically modified mice were maintained as heterozygotes on a C57BL/6J background.

To generate mice in which the *Trpa1* and *Ramp1* genes were conditionally silenced in Schwann cells/oligodendrocytes, homozygous 129S-Trpa1^{tm2Kykw}/J (*floxed TRPA1, Trpa1*$^{fl/fl}$, RRID:IMSR_JAX:008649 Jackson Laboratory) and C57BL/6N-Ramp1$^{<tm1c(EUCOMM)Wtsi>/H}$ (*floxed* Ramp1,

Ramp1$^{fl/fl}$ Stock No: EM:07401, MRC HARWELL Mary Lion Center)[54] were crossed with hemizygous B6.Cg-Tg(Plp1-Cre^{ERT})3Pop/J mice (*Plp1-Cre*^{ERT}, RRID:IMSR_JAX:005975 Jackson Laboratory), expressing a tamoxifen-inducible Cre in myelinating cells (Plp1, proteolipid protein myelin 1)[28]. The progeny (*Plp1-Cre*^{ERT};*Trpa1*$^{fl/fl}$ and *Ramp1-Cre*^{ERT};*Trpa1*$^{fl/fl}$) was genotyped by PCR for *Trpa1, Ramp1* and *Plp1-Cre*^{ERT}. Mice negative for *Plp1-Cre*^{ERT} (*Plp1-Cre*$^{ERT-}$;*Trpa1*$^{fl/fl}$ and *Plp1-Cre*$^{ERT-}$;*Ramp1*$^{fl/fl}$) were used as control. Both positive and negative mice to *Cre*^{ERT} and homozygous for floxed *Trpa1* (*Plp1-Cre*^{ERT};*Trpa1*$^{fl/fl}$ and *Plp1-Cre*$^{ERT-}$;*Trpa1*$^{fl/fl}$, respectively) and floxed *Ramp1 (Plp1-Cre*^{ERT};*Ramp1*$^{fl/fl}$ and *Plp1-Cre*$^{ERT-}$;*Ramp1*$^{fl/fl}$) mice were treated with 4-hydroxytamoxifen (4-OHT) by subcutaneous periorbital (p.orb.) injection (0.02 mg/10 µl in corn oil once a day for 3 consecutive days). Some *Plp1-Cre*^{ERT};*Ramp1*$^{fl/fl}$ and *Plp1-Cre*$^{ERT-}$;*Ramp1*$^{fl/fl}$ mice were treated with intraperitoneal (i.p.) 4-OHT (1 mg/100 µl in corn oil, once a day for 3 consecutive days).

Treatments resulted in Cre-mediated ablation of *Trpa1* and *Ramp1* in PLP-expressing Schwann cells/oligodendrocytes. To selectively delete the *Trpa1* and *Ramp1* gene in primary sensory neurons, *Trpa1*$^{fl/fl}$ and *Ramp1*$^{fl/fl}$ mice were crossed with hemizygous *Advillin-Cre* mice *(Adv-Cre)*[28, 55, 56]. Both positive and negative mice to *Cre*^{ERT} and homozygous for floxed *Trpa1* (*Adv-Cre*$^{+}$;*Trpa1*$^{fl/fl}$ and *Adv-Cre*$^{-}$;*Trpa1*$^{fl/fl}$, respectively) and floxed *Ramp1 (Adv-Cre*$^{+}$;*Ramp1*$^{fl/fl}$ and *Adv-Cre*$^{-}$;*Ramp1*$^{fl/fl}$) were used.

The group size of n = 8 animals for behavioral experiments was determined by sample size estimation using G*Power (v3.1)[57] to detect size effect in a post-hoc test with type 1 and 2 error rates of 5 and 20%, respectively. Mice were allocated to vehicle or treatment groups using a randomization procedure (http://www.randomizer.org/). Investigators were blinded to the identities (genetic background) and treatments, which were revealed only after data collection. No animals were excluded from experiments.

All behavioral experiments were in accordance with European Union (EU) guidelines for animal care procedures and the Italian legislation (DLgs 26/2014) application of the EU Directive 2010/63/EU. Study was approved by the Italian Ministry of Health (research permits #383/2019-PR and #765/2019-PR). The behavioral studies followed the animal research reporting *in vivo* experiment (ARRIVE) guidelines[58]. Mice were housed in a temperature- and humidity-controlled *vivarium* (12 hr dark/light cycle, free access to food and water, 5 animals per cage). At least 1 hr before behavioral experiments, mice were acclimatized to the experimental room and behavior was evaluated between 9:00 am and 5:00 pm. All the procedures were conducted following the current guidelines for laboratory animal care and the ethical guidelines for investigations of experimental pain in conscious animals set by the International Association for the Study of Pain[59]. Animals were anesthetized with a mixture of ketamine and xylazine (90 mg/kg and 3 mg/kg, respectively, i.p.) and euthanized with inhaled CO_2 plus 10–50% O_2.

Cell lines. Primary cultures of human Schwann cells (HSCs, #1700, ScienCell Research Laboratories) were grown and maintained in Schwann cell medium (#1701, ScienCell Research Laboratories) at 37°C in 5% CO_2 and 95% O_2. Cells were passaged at 90% confluency and discarded after 12 passages. HEK293T (#CRL-3216™, American Type Culture Collection) cells were cultured in Dulbecco's Modified Eagle's

Medium (DMEM) supplemented with heat inactivated fetal bovine serum (FBS, 10%), L-glutamine (2 mM), penicillin (100 U/ml) and streptomycin (100 mg/ml) at 37°C in 5% CO_2 and 95% O_2. The mouse Schwann cell line (IMS32 cells, #PMC-SWN-IMS32-COS, Cosmo Bio USA) was grown and maintained in Schwann cell medium (#PMC-SWN-MM-COS, Cosmo Bio USA) at 37°C in 5% CO_2 and 95% O_2[60, 61]. All cells were used when received without further authentication.

Pharmacological reagents. Supplementary Tables 1 and 2 provide doses, routes of administration and concentrations and of all pharmacological reagents.

Behavioral experiments

Treatment protocol. Subcutaneous injections were made in the periorbital area 2-3 mm from the external eyelid corner[17]. Briefly, the mouse was lifted by the base of the tail and placed on a solid surface with one hand and the tail was pulled back. Then, it was quickly and firmly picked up by the scruff of the neck with the thumb and index finger of the other hand. Injection was made rapidly by a single operator with minimal animal restraint. Mice received unilateral (right side) injections (10 µl/site) of CGRP (1.5 nmol in 0.9% NaCl), SP (3.5 nmol in 0.9% NaCl), capsaicin (10, 50, 100 pmol in 0.1% dimethyl sulfoxide, DMSO), or vehicles (control). Mice received bilateral injections (10 µl/site, right side same site as stimulus, left side symmetrical to right side) of antagonists and inhibitors. CGRP (1.5 nmol in 0.9% NaCl) or vehicle was also administered by intraplantar (i.pl., 20 µl/site) or systemic (0.1 mg/kg, i.p.) injection. GTN was administered at 10 mg/kg, i.p. injection.

Acute nociception. Immediately after the p.orb. injection, mice were placed inside a plexiglass chamber and spontaneous nociception was assessed for 10 min by measuring the time (s) that the animal spent rubbing the injected area of the face with its paws[17, 62].

Periorbital mechanical allodynia. PMA was assessed using the up-down paradigm[63, 64] in the same mice in which acute nociceptive responses were monitored. Briefly, mice were placed in a restraint apparatus designed for the evaluation of periorbital mechanical thresholds[17]. One day before the first behavioral observation, mice were habituated to the apparatus. PMA was evaluated in the periorbital region over the rostral portion of the eye (*i.e.*, the area of the periorbital region facing the sphenoidal rostrum)[65] before (basal threshold) and after (0.5, 1, 2, 4, 6, 8 hr) treatments. On the day of the experiment, after 20 min of adaptation inside the chamber, a series of 7 von Frey filaments in logarithmic increments of force (0.02, 0.04, 0.07, 0.16, 0.4, 0.6 and 1.0 g) were applied to the periorbital area perpendicular to the skin, with sufficient force to cause slight buckling, and held for approximately 5 s to elicit a positive response. Mechanical stimuli were applied homolaterally outside the periorbital area at a distance of 6-8 mm from the site where stimuli were injected. The response was considered positive by the following criteria: mouse vigorously stroked its face with the forepaw, head withdrawal from the stimulus, or head shaking.

Mechanical stimulation started with the 0.16 g filament. Absence of response after 5 s led to the use of a filament with increased force, whereas a positive response led to the use of a weaker (*i.e.* lighter) filament. Six measurements were collected for each mouse or until four consecutive positive or negative responses occurred. The 50% mechanical withdrawal threshold (expressed in g) was then calculated from these scores by using a δ value of 0.205, previously determined.

Paw mechanical allodynia. Paw mechanical allodynia was evaluated by measuring the paw withdrawal threshold by using the up-down paradigm[63, 64]. Mice were acclimatized (1 hr) in individual clear plexiglass boxes on an elevated wire mesh platform, to allow for access to the plantar surfaces of the hind paws. von Frey filaments of increasing stiffness (0.07, 0.16, 0.4, 0.6 and 1.0, 1.4 and 2 g) were applied to the hind paw plantar surfaces of mice with enough pressure to bend the filament. The absence of a paw being lifted after 5 s led to the use of the next filament with an increased force, whereas a lifted paw indicated a positive response, leading to the use of a subsequently weaker filament. Six measurements were collected for each mouse or until four consecutive positive or negative responses occurred. The 50% mechanical withdrawal threshold (expressed in g) was then calculated.

Primary culture of mouse Schwann cells. Mouse Schwann cells (MSC) were isolated from sciatic nerves of C57BL/6J, *Trpa1*$^{+/+}$ and *Trpa1*$^{-/-}$, *Plp1-Cre*$^{ERT+}$*;Ramp1*$^{fl/fl}$ and *Plp1-Cre*$^{ERT-}$*;Ramp1*$^{fl/fl}$ mice[28, 66]. The epineurium was removed, and nerve explants were divided into 1 mm segments and dissociated enzymatically using collagenase (0.05%) and hyaluronidase (0.1%) in Hank's Balanced Salt Solution (HBSS, 2 hr, 37 °C). Cells were collected by centrifugation (800 rpm, 10 min, room temperature) and the pellet was resuspended and cultured in DMEM containing fetal calf serum (10%), L-glutamine (2 mM), penicillin (100 U/ml), streptomycin (100 mg/ml), neuregulin (10 nM) and forskolin (2 µM). Three days later, cytosine arabinoside (Ara-C, 10 mM) was added to remove fibroblasts. Cells were cultured at 37 °C in 5% CO_2 and 95% O_2. The culture medium was replaced every 3 days and cells were used after 15 days of culture.

qRT-PCR. Detailed method and the sets of primers for human and mouse cells are reported in Supplementary information and Table S3**.**

Calcium imaging. HSCs, MSCs and IMS32 cells were plated on poly-L-lysine-coated (8.3 µM) 35 mm glass coverslips and maintained at 37 °C in 5% CO_2 and 95% O_2 for 24 hr. Cells were loaded (40 min) with Fura-2 AM-ester (5 µM) added to the buffer solution (37 °C) containing (in mM) 2 $CaCl_2$; 5.4 KCl; 0.4 $MgSO_4$; 135 NaCl; 10 D-glucose; 10 HEPES and bovine serum albumin (BSA, 0.1%) at pH 7.4. Cells were

exposed to CGRP (0.01-10 μM) or vehicle (0.9% NaCl) and the Ca^{2+} response was monitored for approximately 40 min. In another set of experiments, IMS32 cells were exposed to AITC (30 μM) or vehicle (0.03% DMSO). The Ca^{2+} response to CGRP was monitored in the presence of CGRP8-37 (100 nM), olcegepant (100 nM), SQ22536 (100 μM), L-NAME (10 μM), A967079 (50 μM), PBN (50 μM), H89 (1 μM), ML171 (1 μM) or vehicle (0.1 % DMSO), and also in the presence of DIPMA-MK-3207 (1-1000 nM) and MK-3207 free drug (0.01-1000 μM) or DIPMA-empty. Some experiments used Ca^{2+}-free buffer solution containing EDTA (1 mM). Results were expressed as percent increase in $ratio_{340/380}$ over baseline normalized to the maximum effect induced by ionomycin (5 μM) added at the end of each experiment.

Protein extraction and western immunoblot assay. Detailed method is reported in Supplementary information.

In-cell ELISA assay. HSCs or IMS32 cells were plated in 96-well black wall clear bottom plates (Corning Life Sciences) (5×10^5 cells/well) and maintained at 37 °C in 5% CO_2 and 95% O_2 for 24 hr. HSCs and IMS32 cells were exposed to CGRP (1 and 10 μM, respectively) or its vehicle (phosphate buffered saline, PBS) for 5, 10, 15, 30 and 60 min, at 37 °C, then washed with DMEM pH 2.5 and fixed in 4% paraformaldehyde for 30 min. Cells were then washed with TBST (0.05%) and blocked with donkey serum (5%) for 4 hr at room temperature and incubated overnight 4 °C with $eNOS^{pS1177}$ (#ab184154, rabbit polyclonal, 1:100, Abcam). Cells were then washed and incubated with donkey anti-rabbit IgG conjugated with horseradish peroxidase (HRPO, 1:2000, Bethyl Laboratories Inc.) for 2 hr at room temperature. Cells were then washed and stained using SIGMAFAST OPD for 30 min protected from light. After the incubation period, the absorbance was measured at 450 nm. Change in NOS3 phosphorylation was calculated as a percentage of the signal in vehicle-treated cells.

cAMP ELISA assay. cAMP level was determined by the CatchPoint™ cyclic-AMP fluorescent assay kit (#R8088, Molecular Device) according to the manufacturer's protocol. Briefly, HSCs or IMS32 cells were plated in 96-well black wall clear bottom plates (Corning Life Sciences) (5×10^5 cells/well) and maintained in 5% CO_2 and 95% O_2 (24 hr, 37 °C). The cultured medium was replaced with HBSS added with olcegepant (100 nM), CGRP8-37 (100 nM), SQ22536 (100 μM), L-NAME (10 μM) or vehicle (0.1% DMSO in HBSS) for 20 min at room temperature. HSCs or IMS32 cells were then stimulated with CGRP (1 and 10 μM, respectively), forskolin (1 μM, positive control) or their vehicles (HBSS) and maintained for 40 min at room temperature protected from light. Signal was detected 60 min after exposure to the stimuli. cAMP level was calculated using cAMP standards and expressed as nmol/1.

Nitric oxide assay. Nitric oxide was determined by using the fluorometric-orange assay kit (#ab219932, Abcam) according to the manufacturer's protocol. HSCs or IMS32 cells were plated 96-well black wall clear bottom plates (Corning Life Sciences) (5×10^5 cells/well) and maintained in 5% CO_2 and 95% O_2 (24 hr, 37 °C). The cultured medium was replaced with Hanks' balanced salt solution (HBSS) added with olcegepant (100 nM), CGRP8-37 (100 nM), SQ22536 (100 μM), L-NAME (10 μM), A967079 (50 μM), PS2 or Dy4 (both 30 μM), PS2 inact or Dy4 inact (30 μM) or vehicle (0.1% DMSO in HBSS) for 20 min at room temperature. HSCs or IMS32 cells were then stimulated with CGRP (1 and 10 μM, respectively), diethylamine NONOate (1 mM, positive control) or their vehicles (HBSS) and maintained for 40 min at room temperature protected from light. Signal was detected 60 min after exposure to the stimuli. Change in nitric oxide level was calculated as percentage of the vehicle.

H_2O_2 assay. H_2O_2 was determined by using the Amplex Red assay (#A12222, Thermo Fisher Scientific). Detailed method is reported in Supplementary information.

Immunofluorescence. Anesthetized mice were transcardially perfused with PBS and 4% paraformaldehyde. Trigeminal and sciatic nerves were removed, postfixed for 24 hr, and paraffin-embedded. Human and mouse formalin fixed paraffin embedded (FFPE) sections (5 μm) were incubated with primary antibodies: TRPA1 (#ab58844, rabbit polyclonal, 1:400, Abcam), S100 (#ab14849, mouse monoclonal [4B3], 1:300, Abcam), CLR (#NLS6731, rabbit polyclonal, 1:30, Novus Biologicals), RAMP1 (#ab241335, rabbit polyclonal, 1:200, Abcam), diluted in fresh blocking solution (PBS, pH 7.4, 2.5% normal goat serum, [NGS]). Sections were then incubated with the fluorescent polyclonal secondary antibodies Alexa Fluor 488 and 594 (#A32731, #A32727 1:600; Invitrogen), and coverslipped using mounting medium with DAPI (Abcam). The Pearson correlation (Rcoloc) value for RAMP1 and S100 in the colocalization studies were calculated using the colocalization Plugin of the ImageJ software (ImageJ 1.32J, National Institutes of Health). The use of FFPE sections of human abdominal cutaneous tissues was approved by the Local Ethics Committee of the Florence University Hospital (Area Vasta Toscana Centro) (18271_bio/2020), according to the Helsinki Declaration, and informed consent was obtained.

cAMP cADDIS assay. HSCs were plated on poly-D-lysine-coated 96-well black wall clear bottom plates (Corning Life Sciences) (25×10^3 cells/well) and incubated in 5% CO_2 and 95% O_2 for 4-6 hr. HSCs were transduced with the baculovirus mediated Green Upward cADDIS cAMP reporter (25 μl/well, Montana Molecular) following manufacturer's instructions, and cells were incubated in 5% CO_2 and 95% O_2 (48 hr, 37 °C). HSCs were washed twice in HBSS plus HEPES (10 mM) pH 7.4. Cells were incubated in

HBSS/HEPES with the CLR/RAMP1 antagonists olcegepant (100 pM-100 μM) or vehicle (control) for 30 min. Plates were mounted in a FlexStation3 plate reader (Molecular Devices) and fluorescence (485-500 excitation, 515-530 emission with cutoff at 510) was monitored. Baseline was measured for 1 min, and cells were stimulated with human CGRPa (100 pM-10 μM) or forskolin (10 μM, positive control). For single cell imaging, HSCs were plated on poly-D-lysine-coated 35 mm glass bottom dishes (MatTek, Ashland) (40×10^3 cells/dish) and incubated in 5% CO_2 and 95% O_2 (overnight, 37 °C). HSCs cells were transduced with Green Upward cADDIS and incubated for 48 hr. HSCs were washed twice in HBSS/HBS and mounted on a Leica DMI8 microscope (Wetzlar, Germany). Fluorescence (470/40 excitation, 527/30 emission) was measured every 5 s. Baseline was measured for 30 s, and HSCs were challenged with human CGRPa (100 nM). Images were analyzed with ImageJ (NIH). To inhibit endocytosis, cells were incubated in HBSS containing 0.45 M sucrose or normal HBSS (control) for 30 min at 37 °C before cAMP assays.

CAMYEL BRET cAMP assay. HEK293 cells stably expressing the CAMYEL BRET sensor (~$2x10^6$) were seeded into 90 mm Petri dish (Corning™, USA) in DMEM/FBS/Geneticin and incubated in 5% CO_2 and 95% O_2 (24 hr, 37 °C). Prior to the transfection, the medium was changed to fresh DMEM/FBS/Geneticin and rat CLR/RAMP1 was transfected (2.5 μg CLR/RAMP1 DNA/dish) using JetPEI (Polyplus Transfection, France) at a 1:6 ratio. After 24 hr, cells were plated in poly-L-lysine coated black 96 well CulturPlate (Perkin Elmer, USA) and incubated in 5% CO_2 and 95% O_2 (24 hr, 37 °C). BRET was assessed using a LUMIstar (BMG LABTECH, Germany). On the day of the assay, cells were equilibrated in HBSS for 30 min, supplemented with 12 mM HEPES at 37 °C in CO_2-free incubator. DIPMA-MK-3207 or free MK-3207 was incubated for 25 min, followed by the addition of coelentrazine-h (50 μM) for 5 min. Baseline was then measured for 5 min, followed by stimulation with CGRP (100 nM, ~EC_{50}), vehicle (HBSS) or forskolin (1 μM, positive control), and further measurements for 5 min. Buffer was then replaced by HBSS with coelentrazine-h (50 μM) and measurements were resumed for further 25 min.

Synthesis of TAMRA-CGRP and endocytosis of TAMRA-CGRP and Cy5-DIPMA nanoparticles. Detailed method is reported in supplementary information.

EbBRET assays of G protein and βARR recruitment to the plasma membrane and endosomes cDNAs. Detailed method is reported in supplementary information.

Synthesis and Characterization of Nanoparticles. Detailed method is reported in supplementary information.

Statistical analysis. Results are expressed as mean ± standard error of the mean (SEM). For multiple comparisons, a one-way analysis of variance (ANOVA) followed by the post-hoc Bonferroni's test or Dunnett's test was used. Two groups were compared using Student's t-test. For behavioral experiments with repeated measures, the two-way mixed model ANOVA followed by the post-hoc Bonferroni's test was used. Statistical analyses were performed on raw data using Graph Pad Prism 8 (GraphPad Software Inc.). IC_{50} values and confidence intervals were determined from non-linear regression models using Graph Pad Prism 8 (GraphPad Software Inc.). P values less than 0.05 ($P<0.05$) were considered significant. Statistical tests used and the sample size for each analysis are listed in the Fig. legend.

Data Availability. Materials and data generated from this study are available upon request from Pierangelo Geppetti (geppetti@unifi.it) or Nigel W. Bunnett (nwb2@nyu.edu).

Declarations

Acknowledgments

Supported by grants from European Research Council (ERC) under the European Union's Horizon 2020 research and innovation programme (grant agreement No. 835286) (P.G.); National Institutes of Health (NS102722, DE026806, DK118971, DE029951, N.W.B., B.L.S.) and Department of Defense (W81XWH1810431, N.W.B., B.L.S.).

Author Contributions

F.D.L., R.N., A.H., L.L., D.D.J., R.L., J.D., M.M., D.S.M.d A., P.R-G, M.W., J.R., A.I., N.V., T.P.D., B.L.S., N.W.B., P.G., designed and conducted the experiments, performed the analysis, discussed the results, and wrote the paper.

Competing interests statement

N.W.B. is a founding scientist of Endosome Therapeutics Inc. P.G. is a member of the Scientific Advisory Board of Endosome Therapeutics Inc. R.N., F.D.L. and P.G. are founding scientists of FloNext Srl. P.G. has been in advisory boards and/or received fees for lectures from Novartis, Amgen, TEVA, AbbVie.

References

1. Lewis T. Experiments Relating to Cutaneous Hyperalgesia and Its Spread Through Somatic Nerves. *Clin Sci* **2**, 373–414 (1936).
2. Russell FA, King R, Smillie SJ, Kodji X, Brain SD. Calcitonin gene-related peptide: physiology and pathophysiology. *Physiol Rev* **94**, 1099–1142 (2014).

3. Geppetti P, Holzer P. *Neurogenic Inflammation*. Boca Raton (1996).
4. Szallasi A, Blumberg PM. Vanilloid (Capsaicin) receptors and mechanisms. *Pharmacol Rev* **51**, 159–212 (1999).
5. Steinhoff MS, von Mentzer B, Geppetti P, Pothoulakis C, Bunnett NW. Tachykinins and their receptors: contributions to physiological control and the mechanisms of disease. *Physiol Rev* **94**, 265–301 (2014).
6. La JH, Wang J, Bittar A, Shim HS, Bae C, Chung JM. Differential involvement of reactive oxygen species in a mouse model of capsaicin-induced secondary mechanical hyperalgesia and allodynia. *Mol Pain* **13**, 1744806917713907 (2017).
7. Schmelz M, Luz O, Averbeck B, Bickel A. Plasma extravasation and neuropeptide release in human skin as measured by intradermal microdialysis. *Neurosci Lett* **230**, 117–120 (1997).
8. Ali Z, Meyer RA, Campbell JN. Secondary hyperalgesia to mechanical but not heat stimuli following a capsaicin injection in hairy skin. *Pain* **68**, 401–411 (1996).
9. Sinclair SR, *et al.* Inhibition of capsaicin-induced increase in dermal blood flow by the oral CGRP receptor antagonist, telcagepant (MK-0974). *Br J Clin Pharmacol* **69**, 15–22 (2010).
10. Olesen J, *et al.* Calcitonin gene-related peptide receptor antagonist BIBN 4096 BS for the acute treatment of migraine. *N Engl J Med* **350**, 1104–1110 (2004).
11. Ashina H. Migraine. *N Engl J Med* **383**, 10 (2020).
12. Doods H, Arndt K, Rudolf K, Just S. CGRP antagonists: unravelling the role of CGRP in migraine. *Trends Pharmacol Sci* **28**, 580–587 (2007).
13. Hostetler ED, *et al.* In vivo quantification of calcitonin gene-related peptide receptor occupancy by telcagepant in rhesus monkey and human brain using the positron emission tomography tracer [11C]MK-4232. *J Pharmacol Exp Ther* **347**, 478–486 (2013).
14. Noseda R, *et al.* Fluorescently-labeled fremanezumab is distributed to sensory and autonomic ganglia and the dura but not to the brain of rats with uncompromised blood brain barrier. *Cephalalgia* **40**, 229–240 (2020).
15. Mogil JS, *et al.* Variable sensitivity to noxious heat is mediated by differential expression of the CGRP gene. *Proc Natl Acad Sci U S A* **102**, 12938–12943 (2005).
16. Rea BJ, *et al.* Peripherally administered calcitonin gene-related peptide induces spontaneous pain in mice: implications for migraine. *Pain* **159**, 2306–2317 (2018).
17. De Logu F, *et al.* Migraine-provoking substances evoke periorbital allodynia in mice. *J Headache Pain* **20**, 18 (2019).
18. Marone IM, *et al.* TRPA1/NOX in the soma of trigeminal ganglion neurons mediates migraine-related pain of glyceryl trinitrate in mice. *Brain* **141**, 2312–2328 (2018).
19. Ashina M, Hansen JM, BO AD, Olesen J. Human models of migraine - short-term pain for long-term gain. *Nat Rev Neurol* **13**, 713–724 (2017).
20. Lipton RB, *et al.* Cutaneous allodynia in the migraine population. *Ann Neurol* **63**, 148–158 (2008).

21. Burstein R, Yarnitsky D, Goor-Aryeh I, Ransil BJ, Bajwa ZH. An association between migraine and cutaneous allodynia. *Annals of Neurology* **47**, 614–624 (2000).
22. McLatchie LM, *et al.* RAMPs regulate the transport and ligand specificity of the calcitonin-receptor-like receptor. *Nature* **393**, 333–339 (1998).
23. Lennerz JK, *et al.* Calcitonin receptor-like receptor (CLR), receptor activity-modifying protein 1 (RAMP1), and calcitonin gene-related peptide (CGRP) immunoreactivity in the rat trigeminovascular system: differences between peripheral and central CGRP receptor distribution. *J Comp Neurol* **507**, 1277–1299 (2008).
24. Beckers HJ, Klooster J, Vrensen GF, Lamers WP. Ultrastructural identification of trigeminal nerve terminals in the pterygopalatine ganglion of rats: an anterograde tracing and immunohistochemical study. *Brain Res* **557**, 22–30 (1991).
25. Cheng L, Khan M, Mudge AW. Calcitonin gene-related peptide promotes Schwann cell proliferation. *J Cell Biol* **129**, 789–796 (1995).
26. Edvinsson JCA, *et al.* C-fibers may modulate adjacent Adelta-fibers through axon-axon CGRP signaling at nodes of Ranvier in the trigeminal system. *J Headache Pain* **20**, 105 (2019).
27. Toth CC, *et al.* Locally synthesized calcitonin gene-related Peptide has a critical role in peripheral nerve regeneration. *J Neuropathol Exp Neurol* **68**, 326–337 (2009).
28. De Logu F, *et al.* Schwann cell TRPA1 mediates neuroinflammation that sustains macrophage-dependent neuropathic pain in mice. *Nat Commun* **8**, 1887 (2017).
29. De Logu F, *et al.* Peripheral Nerve Resident Macrophages and Schwann Cells Mediate Cancer-induced Pain. *Cancer Res*, (2021).
30. Abdo H, *et al.* Specialized cutaneous Schwann cells initiate pain sensation. *Science* **365**, 695–699 (2019).
31. Jensen DD, *et al.* Neurokinin 1 receptor signaling in endosomes mediates sustained nociception and is a viable therapeutic target for prolonged pain relief. *Sci Transl Med* **9**, (2017).
32. Ramírez-García PD, *et al.* A pH-responsive nanoparticle targets the neurokinin 1 receptor in endosomes to prevent chronic pain. *Nat Nanotechnol* **14**, 1150–1159 (2019).
33. Yarwood RE, *et al.* Endosomal signaling of the receptor for calcitonin gene-related peptide mediates pain transmission. *Proc Natl Acad Sci U S A* **114**, 12309–12314 (2017).
34. Talavera K, *et al.* Mammalian Transient Receptor Potential TRPA1 Channels: From Structure to Disease. *Physiol Rev* **100**, 725–803 (2020).
35. Lassen LH, Haderslev P, Jacobsen VB, Iversen HK, Sperling B, Olesen J. CGRP may play a causative role in migraine. *Cephalalgia* **22**, 54–61 (2002).
36. Guo S, *et al.* Selectivity of commonly used inhibitors of clathrin-mediated and caveolae-dependent endocytosis of G protein–coupled receptors. *Biochimica et Biophysica Acta (BBA) - Biomembranes* **1848**, 2101–2110 (2015).

37. Hosaka K, Rayner SE, von der Weid PY, Zhao J, Imtiaz MS, van Helden DF. Calcitonin gene-related peptide activates different signaling pathways in mesenteric lymphatics of guinea pigs. *Am J Physiol Heart Circ Physiol* **290**, H813-822 (2006).
38. Miyamoto T, Dubin AE, Petrus MJ, Patapoutian A. TRPV1 and TRPA1 mediate peripheral nitric oxide-induced nociception in mice. *PLoS One* **4**, e7596 (2009).
39. Bhattacharya MR, Bautista DM, Wu K, Haeberle H, Lumpkin EA, Julius D. Radial stretch reveals distinct populations of mechanosensitive mammalian somatosensory neurons. *Proc Natl Acad Sci U S A* **105**, 20015–20020 (2008).
40. De Logu F, *et al.* Schwann cells expressing nociceptive channel TRPA1 orchestrate ethanol-evoked neuropathic pain in mice. *J Clin Invest* **129**, 5424–5441 (2019).
41. Farokhzad OC, Langer R. Impact of nanotechnology on drug delivery. *ACS nano* **3**, 16–20 (2009).
42. LaMotte RH, Shain CN, Simone DA, Tsai EF. Neurogenic hyperalgesia: psychophysical studies of underlying mechanisms. *J Neurophysiol* **66**, 190–211 (1991).
43. Melo-Carrillo A, *et al.* Fremanezumab-A Humanized Monoclonal Anti-CGRP Antibody-Inhibits Thinly Myelinated (Adelta) But Not Unmyelinated (C) Meningeal Nociceptors. *J Neurosci* **37**, 10587–10596 (2017).
44. Murinson BB, Hoffman PN, Banihashemi MR, Meyer RA, Griffin JW. C-fiber (Remak) bundles contain both isolectin B4-binding and calcitonin gene-related peptide-positive axons. *J Comp Neurol* **484**, 392–402 (2005).
45. Ziegler EA, Magerl W, Meyer RA, Treede RD. Secondary hyperalgesia to punctate mechanical stimuli. Central sensitization to A-fibre nociceptor input. *Brain* **122** (**Pt 12**), 2245–2257 (1999).
46. Irannejad R, *et al.* Conformational biosensors reveal GPCR signalling from endosomes. *Nature* **495**, 534–538 (2013).
47. Lazar AM, *et al.* G protein-regulated endocytic trafficking of adenylyl cyclase type 9. *Elife* **9**, (2020).
48. Peng GE, Pessino V, Huang B, von Zastrow M. Spatial decoding of endosomal cAMP signals by a metastable cytoplasmic PKA network. *Nat Chem Biol*, (2021).
49. Olesen J, Burstein R, Ashina M, Tfelt-Hansen P. Origin of pain in migraine: evidence for peripheral sensitisation. *Lancet Neurol* **8**, 679–690 (2009).
50. Mullin K, *et al.* Potential for treatment benefit of small molecule CGRP receptor antagonist plus monoclonal antibody in migraine therapy. *Neurology* **94**, e2121-e2125 (2020).
51. Luo G, *et al.* Discovery of (5S,6S,9R)-5-amino-6-(2,3-difluorophenyl)-6,7,8,9-tetrahydro-5H-cyclohepta[b]pyri din-9-yl 4-(2-oxo-2,3-dihydro-1H-imidazo[4,5-b]pyridin-1-yl)piperidine-1-carboxylate (BMS-927711): an oral calcitonin gene-related peptide (CGRP) antagonist in clinical trials for treating migraine. *J Med Chem* **55**, 10644–10651 (2012).
52. Manoukian R, Sun H, Miller S, Shi D, Chan B, Xu C. Effects of monoclonal antagonist antibodies on calcitonin gene-related peptide receptor function and trafficking. *J Headache Pain* **20**, 44 (2019).

53. Kwan KY, *et al.* TRPA1 contributes to cold, mechanical, and chemical nociception but is not essential for hair-cell transduction. *Neuron* **50**, 277–289 (2006).
54. Skarnes WC, *et al.* A conditional knockout resource for the genome-wide study of mouse gene function. *Nature* **474**, 337–342 (2011).
55. Guan Z, *et al.* Injured sensory neuron-derived CSF1 induces microglial proliferation and DAP12-dependent pain. *Nat Neurosci* **19**, 94–101 (2016).
56. Zurborg S, *et al.* Generation and characterization of an Advillin-Cre driver mouse line. *Mol Pain* **7**, 66 (2011).
57. Faul F, Erdfelder E, Lang AG, Buchner A. G*Power 3: a flexible statistical power analysis program for the social, behavioral, and biomedical sciences. *Behav Res Methods* **39**, 175–191 (2007).
58. Kilkenny C, Browne WJ, Cuthill IC, Emerson M, Altman DG. Improving bioscience research reporting: the ARRIVE guidelines for reporting animal research. *PLoS Biol* **8**, e1000412 (2010).
59. Zimmermann M. Ethical guidelines for investigations of experimental pain in conscious animals. *Pain* **16**, 109–110 (1983).
60. Watabe K, Fukuda T, Tanaka J, Honda H, Toyohara K, Sakai O. Spontaneously immortalized adult mouse Schwann cells secrete autocrine and paracrine growth-promoting activities. *J Neurosci Res* **41**, 279–290 (1995).
61. Watabe K, *et al.* Tissue culture methods to study neurological disorders: establishment of immortalized Schwann cells from murine disease models. *Neuropathology* **23**, 68–78 (2003).
62. Luccarini P, Childeric A, Gaydier AM, Voisin D, Dallel R. The orofacial formalin test in the mouse: a behavioral model for studying physiology and modulation of trigeminal nociception. *J Pain* **7**, 908–914 (2006).
63. Dixon WJ. Efficient analysis of experimental observations. *Annu Rev Pharmacol Toxicol* **20**, 441–462 (1980).
64. Chaplan SR, Bach FW, Pogrel JW, Chung JM, Yaksh TL. Quantitative assessment of tactile allodynia in the rat paw. *J Neurosci Methods* **53**, 55–63 (1994).
65. Elliott MB, Oshinsky ML, Amenta PS, Awe OO, Jallo JI. Nociceptive neuropeptide increases and periorbital allodynia in a model of traumatic brain injury. *Headache* **52**, 966–984 (2012).
66. Tao Y. Isolation and culture of Schwann cells. *Methods Mol Biol* **1018**, 93–104 (2013).

Figures

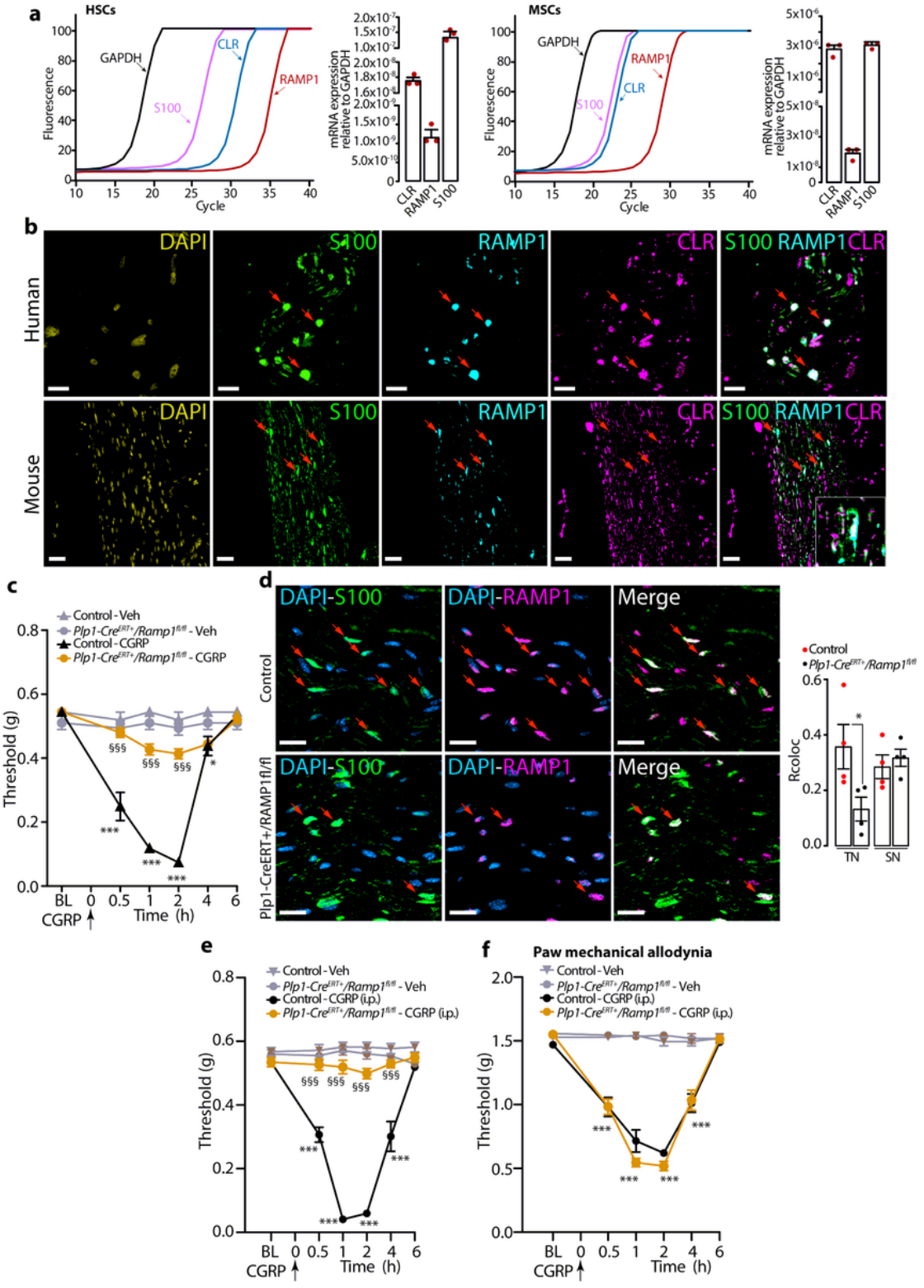

Figure 1

Schwann cell RAMP1 mediates PMA evoked by CGRP. (a) Representative real-time PCR plot and cumulative data for GAPDH, S100, CLR and RAMP1 mRNA in HSCs and MSCs (n=3 independent experiments). (b) Representative images of DAPI and immunoreactive S100, RAMP1 and CLR in human and mouse cutaneous nerve bundles (scale, 10 µm human, 50 µm mouse) (n=3 subjects). (c) PMA induced by CGRP (1.5 nmol) or vehicle in Plp1-CreERT+/Ramp1fl/fl and Control mice (n=8 mice per

group) treated with periorbital 4-OHT. (d) Representative images and colocalization value (Rcoloc) of S100 and RAMP1 in periorbital nerve and sciatic nerve trunks from Plp1-CreERT+;Ramp1fl/fl and Control mice (scale: 20 μm) (n=3 replicates). TN (trigeminal nerve), SN (sciatic nerve). (e) PMA and (f) paw mechanical allodynia induced by intraperitoneal (i.p.) CGRP (0.1 mg/kg) or vehicle in Plp1-CreERT+/Ramp1fl/fl and Control mice (n=8 mice per group) treated with periorbital 4-OHT. Mean±SEM. *P<0.05, ***P<0.001 vs. Control-Veh and TN-Control, §§§P<0.001. vs. Control-CGRP. 2-way (c,e,f) or 1-way (d) ANOVA, Bonferroni correction.

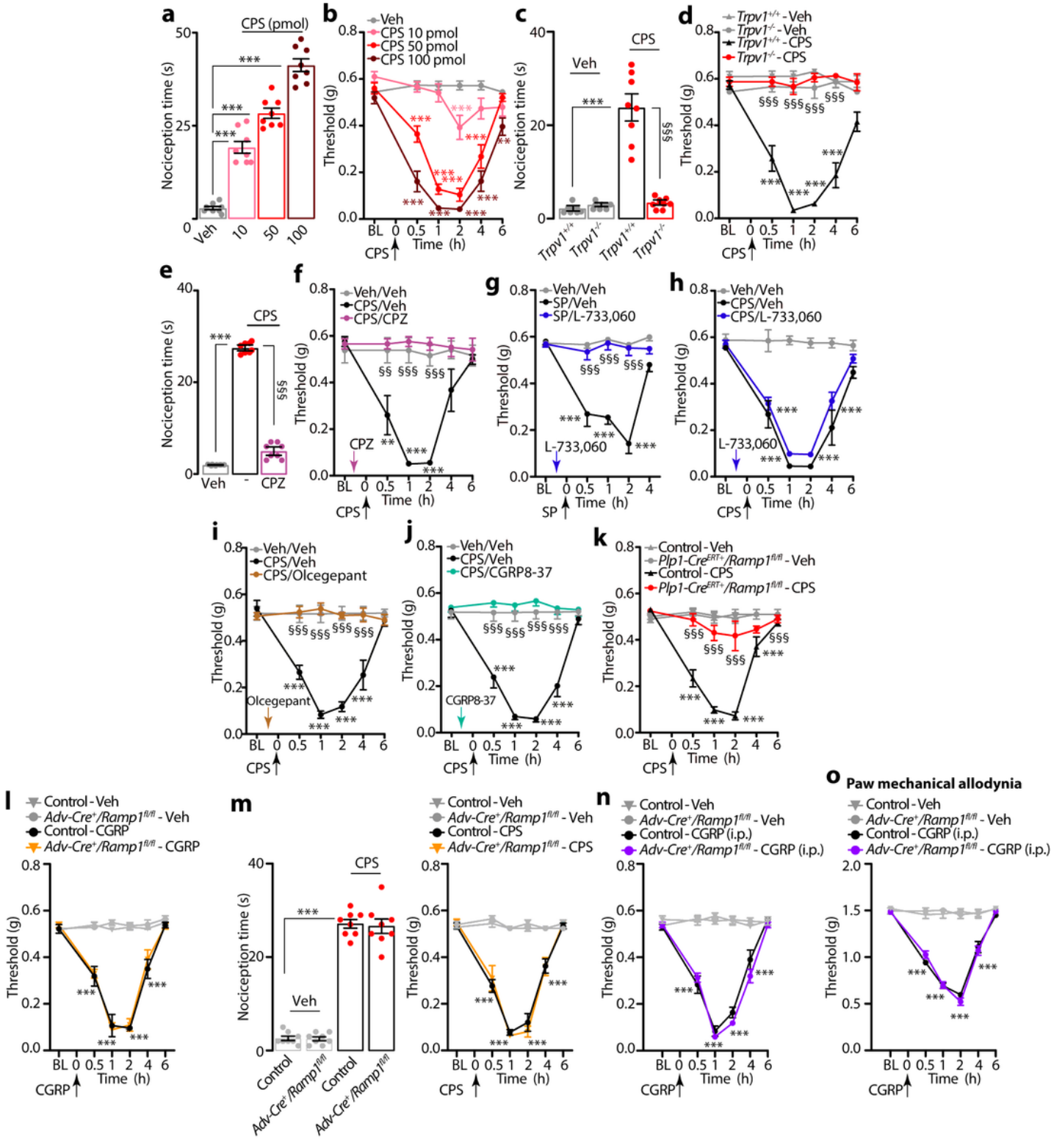

Figure 2

Capsaicin induces PMA via CGRP and CLR/RAMP1 in Schwann cells. (a) Acute nociception and (b) PMA after periorbital injection of capsaicin (CPS, 50 pmol) or vehicle in C57BL/6J mice. (c) Acute nociception and (d) PMA after CPS (50 pmol) or vehicle in Trpv1+/+ and Trpv1−/− mice. (e) Acute nociception and (f) PMA after CPS (50 pmol) or vehicle in C57BL/6J mice pretreated with capsazepine (CPZ, 100 pmol) or vehicle. (g, h) PMA after periorbital SP (3.5 nmol), CPS (50 pmol) or vehicle in C57BL/6J mice pretreated (0.5 h) with L-733,060 (20 nmol) or vehicle. (i, j) PMA after CPS (50 pmol) or vehicle in C57BL/6J mice pretreated (0.5 h) with olcegepant (1 nmol) or CGRP8-37 (10 nmol) or vehicle. (k) PMA after CPS (50 pmol) or vehicle in Plp1-CreERT+/Ramp1fl/fl or Control mice treated with periorbital 4-OHT or vehicle. (l) PMA after periorbital CGRP (1.5 nmol) or vehicle and (m) acute nociceptive response and PMA after periorbital CPS (50 pmol) or vehicle in Adv-Cre+/Ramp1fl/fl or Control mice. (n) PMA and (o) paw mechanical allodynia induced by intraperitoneal (i.p.) CGRP (0.1 mg/kg) or vehicle in Adv-Cre+/Ramp1fl/fl or Control mice. Mean±SEM., n=8 mice per group. **P<0.01, ***P<0.001 vs. Veh/Veh, Trpv1+/+-Veh and Control-Veh; §§P<0.01, §§§P<0.001 vs. Trpv1+/+-CPS, CPS/Veh, SP/Veh, Control-CPS, Control-CGRP. 1-way (a, c, e and m left panel) or 2-way (b, d, f-l, m right panel and n, o) ANOVA, Bonferroni correction.

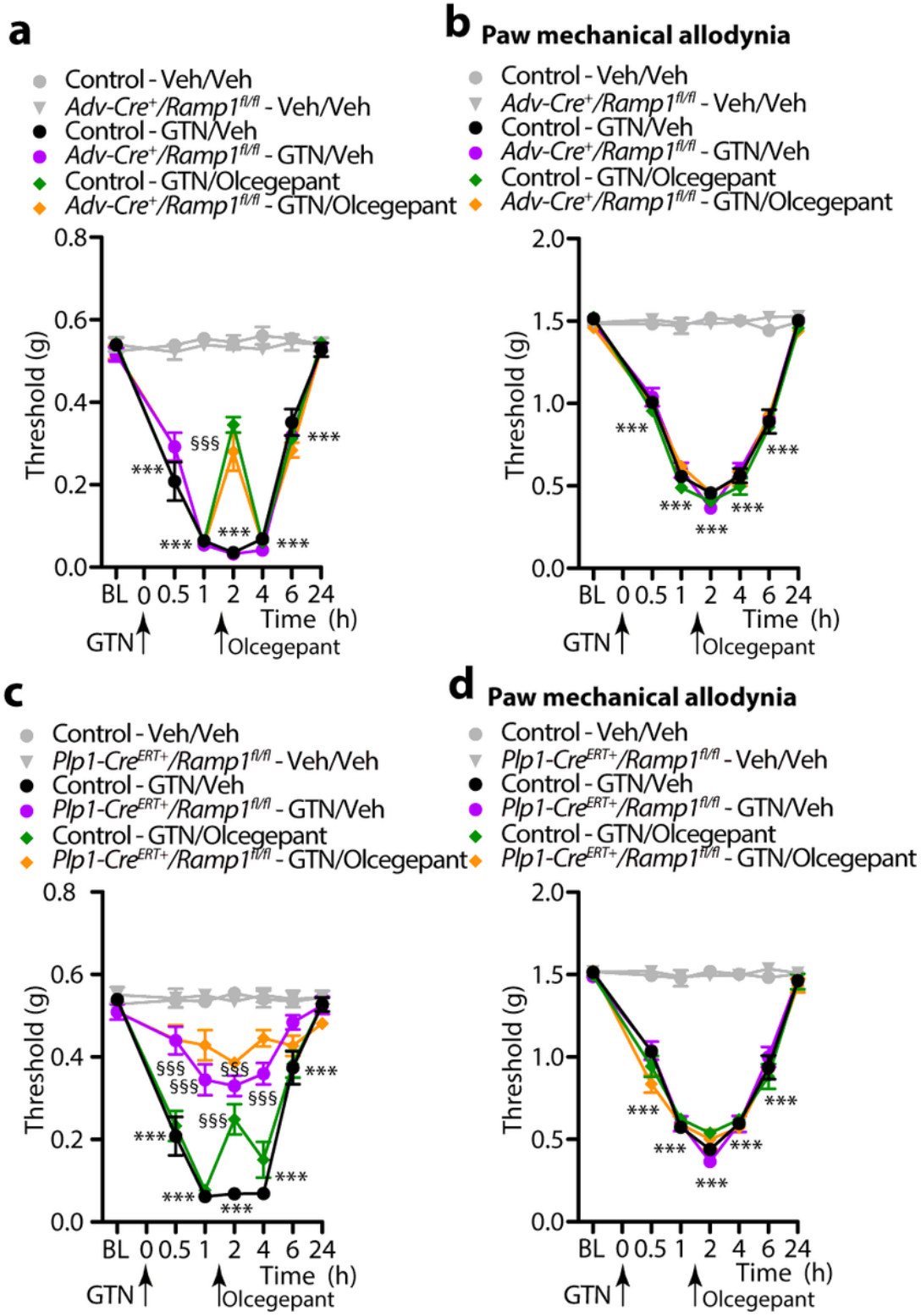

Figure 3

GTN induces PMA via CGRP released from periorbital trigeminal terminals and, CLR/RAMP1 in Schwann cells. (a) PMA and (b) paw mechanical allodynia induced by intraperitoneal (i.p.) GTN (10 mg/kg) or vehicle in Adv-Cre+/Ramp1fl/fl or Control mice post-treated (1.5 hs after GTN) with olcegepant (1 nmol) or vehicle. (c) PMA and (d) paw mechanical allodynia induced by GTN (10 mg/kg, i.p.) or vehicle in Plp1-CreERT+/Ramp1fl/fl or Control (treated with periorbital 4-OHT or vehicle) post-treated (1.5 hs after GTN)

with olcegepant (1 nmol) or vehicle. Mean±SEM., n=8 mice per group. ***P<0.001 vs. Control-Veh/Veh; §§§P<0.001 vs. Control-GTN/Veh. 2-way ANOVA, Bonferroni correction.

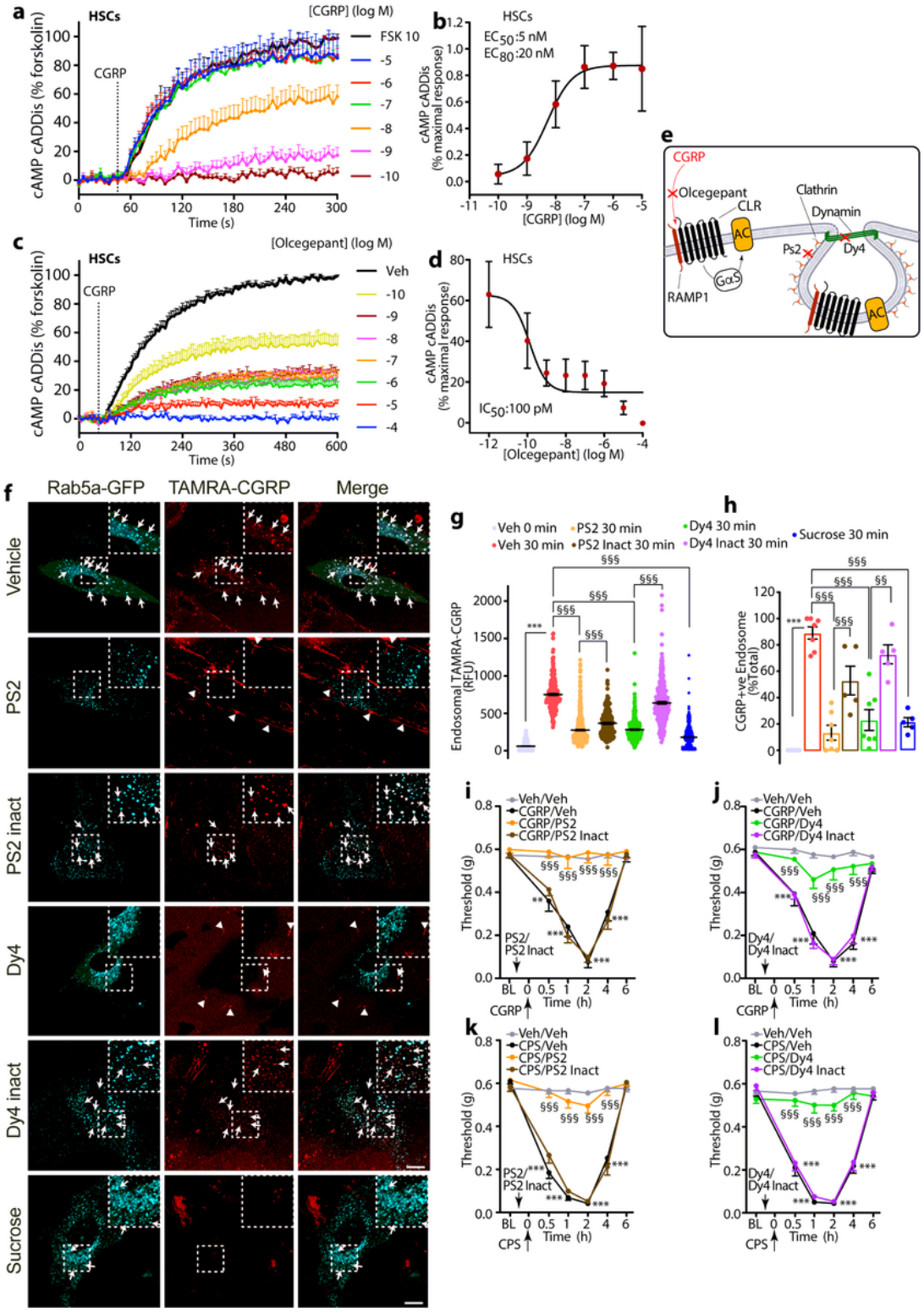

Figure 4

Functional CLR/RAMP1 is expressed by HSCs and undergoes clathrin- and dynamin-mediated endocytosis, which underlies nociception. (a, b) Effects of graded concentrations of CGRP on cAMP formation. (c, d) Effects of graded concentrations of olcegepant on CGRP (100 nM)-evoked cAMP

formation. (e) Pharmacological targets. (f) Representative images of HSCs expressing Rab5a-GFP at 30 min after incubation with TAMRA-CGRP (100 nM). Arrows denote colocalization of TAMRA-CGRP and Rab5a-GFP. Arrowheads denote retention of a weak TAMRA-CGRP signal at the plasma membrane. Cells were preincubated with vehicle, Dyngo-4a (Dy4), Pitstop 2 (PS2), inactive analogs (PS2 and Dy4 inact) (all 30 μM) or sucrose (0.45 M). (n=4 independent experiments). Scale: 10 μm. (g, h) Quantification of localization of TAMRA-CGRP in endosomes (g) and of the number of TAMRA-CGRP+ve endosomes (h). (n=5-7 independent experiments, 5 cells imaged per experiment). (I-L) PMA induced by periorbital CGRP (1.5 nmol) (I, J) or capsaicin (CPS, 50 pmol) (k, l) or vehicle in C57BL/6J mice pretreated (0.5 h) with PS2, Dy4, PS2 or Dy4 inact (all 500 pmol) (n=8 mice per group). Mean±SEM. **P<0.01, ***P<0.001 vs. Veh 0 min, and Veh/Veh; §§P<0.01, §§§P<0.001 vs. Veh 30 min, PS2 30 min, Dy4 30 min, CGRP/PS2 inact, CGRP/Dy4 inact, CPS/PS2 inact, CPS/Dy4 inact. 1-way (h, i) or 2-way (j-m) ANOVA, Bonferroni correction.

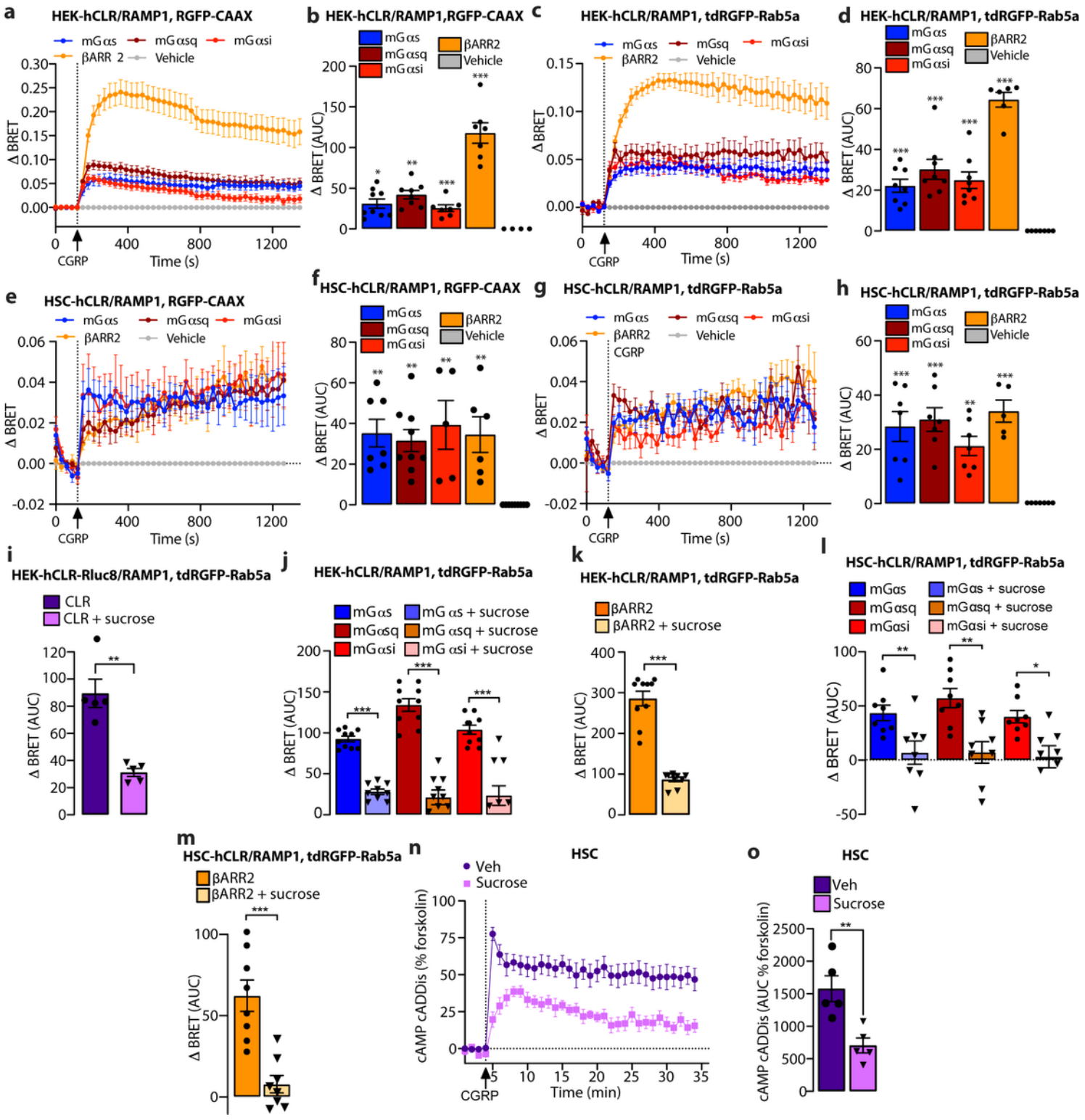

Figure 5

CGRP leads to Gα protein activation and βARR2 recruitment at the plasma membrane and in early endosomes in HEK-hCLR/RAMP1 cells and HSCs-hCLR/RAMP1. Endosomal signaling generates sustained formation of cAMP in HSCs. (a-d) CGRP (100 nM) increased EbBRET between Rluc8-mGαs, Rluc8-mGαsq, Rluc8-mGαsi, and Rluc2-βARR2 with RGFP-CAAX (a, b) and tdRGFP-Rab5a (c, d) in HEK-hCLR/RAMP1 cells. a, c time course. b, d area under curve (AUC). (E-H) CGRP (100 nM) increased EbBRET

between Rluc8-mGαs, Rluc8-mGαsq, Rluc8-mGαsi, and Rluc2-βARR2 with RGFP-CAAX (e, f) and tdRGFP-Rab5a (g, h) in HSC-hCLR/RAMP1 cells. e, g time course. f, h AUC. (i) Hypertonic sucrose (0.45 M) inhibited CGRP (100 nM)-stimulated EbBRET between hCLR-Rluc8 and tdRGFP-Rab5a in HEK-hCLR/RAMP1 cells. (j, k) Hypertonic sucrose (0.45 M) inhibited CGRP (100 nM)-stimulated EbBRET between Rluc8-mGαs, Rluc8-mGαsq, Rluc8-mGαsi and Rluc2-βARR2 with tdRGFP-Rab5a in HEK-hCLR/RAMP1 cells. (l, m) Sucrose (0.45 M) inhibited CGRP (100 nM)-stimulated EbBRET between Rluc8-mGαs, Rluc8-mGαsq, Rluc8-mGαsi, and Rluc2-βARR2 with tdRGFP-Rab5a in HSC-hCLR/RAMP1 cells. (n, o) Sucrose (0.45 M) inhibited CGRP (100 nM)-stimulated formation of cAMP in HSCs. n, time course. o, AUC. Mean±SEM. (n=5-10 independent experiments). *P<0.05, **P<0.01, ***P<0.001, vs. Veh. 1-way ANOVA, Dunnett's correction (b, d, f, h) or parametric unpaired t test (i-m, o).

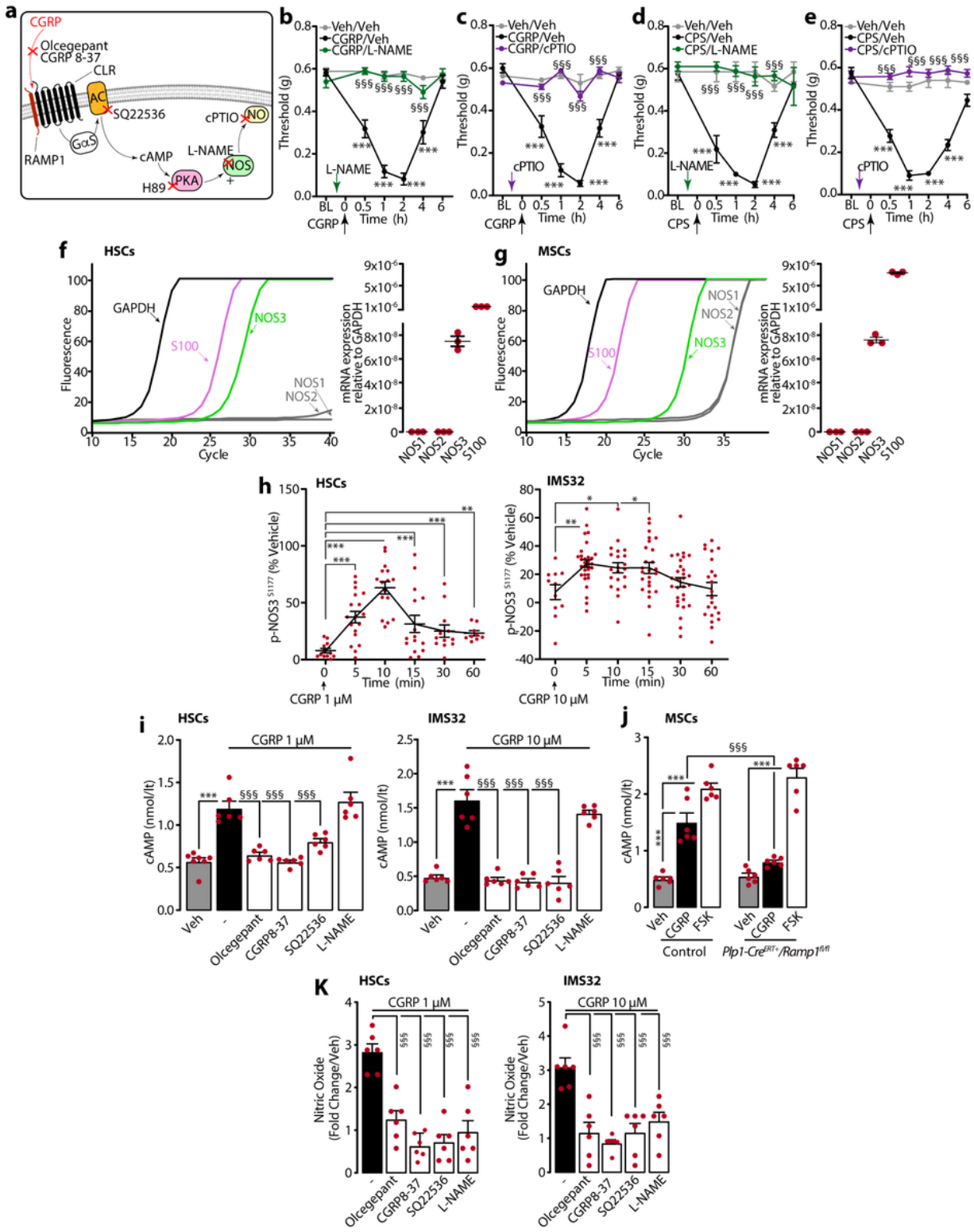

Figure 6

Endogenous and exogenous CGRP induces PMA via NO production. (a) Pharmacological targets. (b-e) PMA after periorbital injection of CGRP (1.5 nmol), capsaicin (CPS, 50 pmol) or vehicle in C57BL/6J mice pretreated (0.5 h) with L-NAME (1 µmol) and cPTIO (200 nmol) or vehicle (n=8 mice per group). (f, g) Real-time PCR plot and cumulative data for GAPDH, S100, NOS1, NOS2 and NOS3 in primary HSCs and MSCs (n=3 independent experiments). (h) In-cell p-NOS3s1177 ELISA in HSCs and IMS32 cells before (0) or

after CGRP (1 μM) (n=4 independent experiments). cAMP assay in (i) HSCs, IMS32 and (j) MSCs from Plp1-CreERT+/Ramp1fl/fl or Control mice treated with intraperitoneal 4-OHT (k) nitric oxide assay in HSCs and IMS32 cells treated with CGRP (1 μM) or vehicle. Some cells were treated with olcegepant (1 μM), CGRP8-37 (1 μM), SQ22536 (100 μM), L-NAME (100 μM) or vehicle (n=3 independent experiments). Mean±SEM. (-) represents the combination of different vehicles. *P<0.05, **P<0.01, ***P<0.001 vs. Veh/Veh, time 0 (min); §§§P<0.001 vs. CGRP/Veh, CGRP 1μM and 10 μM. 1-way (h-k) or 2-way (b-e) ANOVA, Bonferroni correction.

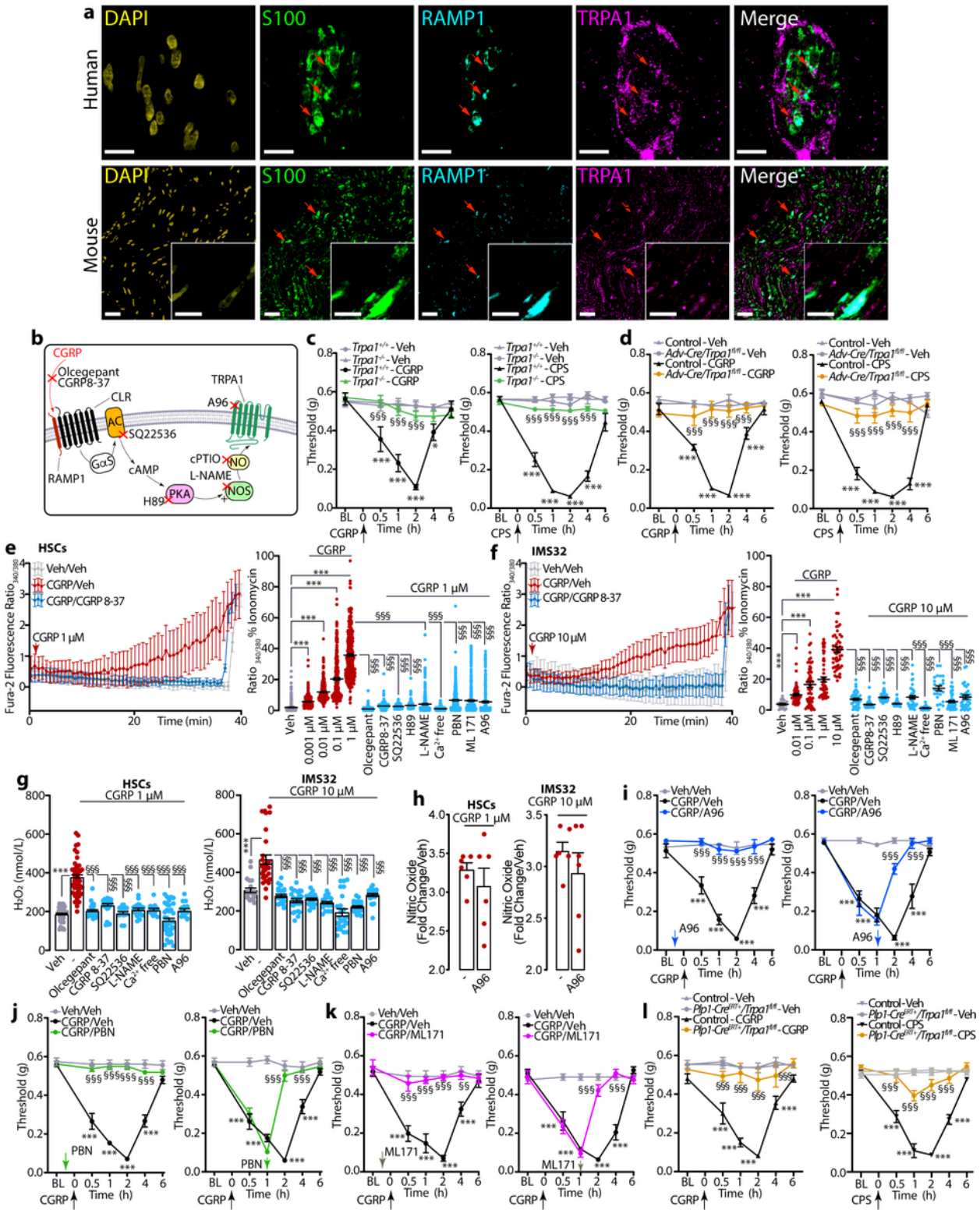

Figure 7

CGRP induces ROS release via Schwann cell TRPA1 activation. (a) Representative images of localization of immunoreactive DAPI, S100, RAMP1 and TRPA1 in human abdominal and mouse periorbital cutaneous nerve bundles (Scale: 10 µm human, 50 µm mouse, inset 10 µm) (n=3 subjects). (b) Pharmacological targets. (c, d) PMA after periorbital injection of CGRP (1.5 nmol), capsaicin (CPS, 50 pmol) or vehicles in (c) Trpa1+/+ and Trpa1-/- mice and in (d) Adv-Cre+/Trpa1fl/fl or Control mice (n=8 mice per group). (e, f) Ca2+ response in HSCs and IMS32 cells exposed to CGRP (10 µM) in the presence of olcegepant (100 nM), CGRP8-37 (100 nM), SQ22536 (100 µM), H89 (1 µM), L-NAME (10 µM), Ca2+-free medium, PBN (50 µM), ML171 (1 µM), A967079 (A96, 50 µM) or vehicle (n=4 independent experiments). (g) H2O2 release in HSCs and IMS32 cells exposed to CGRP (10 µM) in the presence of olcegepant (100 nM), CGRP8-37 (100 nM), SQ22536 (100 µM), L-NAME (10 µM), Ca2+-free medium, PBN (50 µM), A96 (50 µM), or vehicle (0.1 % DMSO) (n=3 independent experiments). (h) Nitric oxide release in HSCs and IMS32 cells exposed to CGRP (1 or 10 µM) in the presence of A96 (50 µM) or vehicle (n=3 independent experiments). (i-k) PMA after CGRP (1.5 nmol) or vehicle in C57BL/6J mice pre-treated (0.5 h, left) or post-treated (1h, right) with (i) A96 (300 nmol), (j) PBN (670 nmol) or (k) ML171 (250 nmol) or vehicle (n=8 mice per group). (l) PMA after CGRP (1.5 nmol), CPS (50 pmol) or vehicles in Plp1-CreERT+/Trpa1fl/fl or Control mice treated with 4-OHT (n=8 mice per group). Mean±SEM. (-) represents the combination of different vehicles. ***P<0.001 vs. Trpa1+/+-Veh, Control-Veh, Veh and Veh/Veh; §§P<0.01, §§§P<0.001 vs. Trpa1+/+-CGRP, Trpa1+/+-CPS, Control-CGRP, Control-CPS, CGRP 1 µM and 1 µM, CGRP/Veh. 2-way (c, d, i-l) or 1-way (e-h) ANOVA, Bonferroni correction.

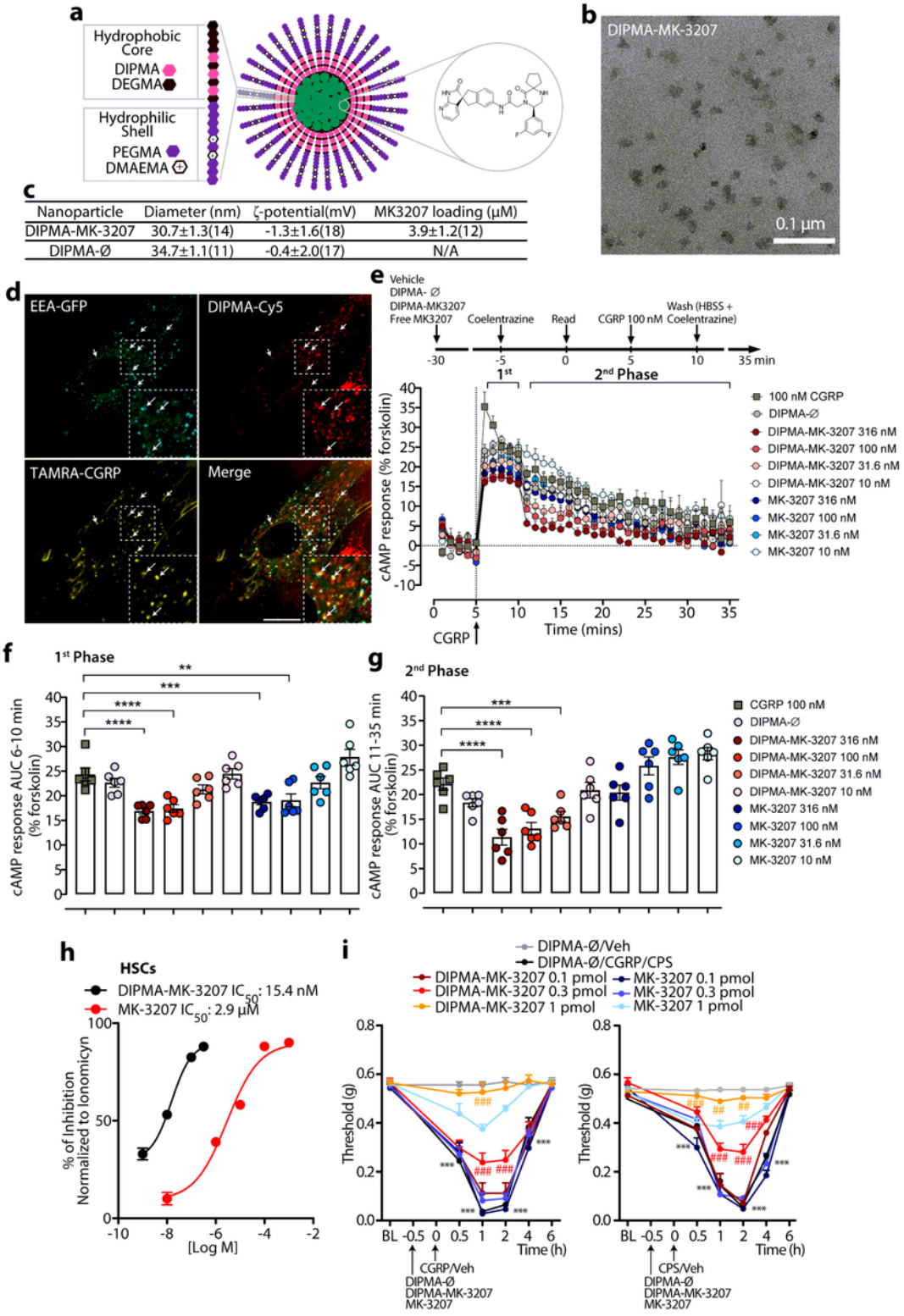

Figure 8

DIPMA-MK-3207 nanoparticles target endosomal CLR/RAMP1 signaling and provide superior relief from CGRP-evoked PMA. (a) pH-responsive DIPMA-MK-3207. (b) Transmission electron micrograph image of DIPMA-MK-3207 (Scale: 0.1 µm). (c) Physicochemical properties of DIPMA-MK-3207 and DIPMA-Ø. (d) Uptake of DIPMA-Cy5 into HSCs expressing EEA1-GFP. Cells were preincubated with DIPMA-Cy5 (40-60 ng/ml) for 30 min and were then incubated with TAMRA-CGRP (100 nM) for 30 min. Arrows denote

accumulation of TAMRA-CGRP in early endosomes containing DIPMA-Cy5. Representative images from n=5 independent experiments (Scale: 10 µm). (e-g). Effects of DIPMA-MK-3207, MK-3207, DIPMA-Ø or vehicle on CGRP- (100 nM) stimulated cAMP formation in HEK-rCLR/RAMP1 cells. (e) Time course and (f, g) integrated response (AUC, area under curve) before (1st phase) and after (2nd phase) washing to remove extracellular CGRP. (h) Concentration-response curves of the inhibition by DIPMA-MK-3207 or free MK-3207 on the Ca2+ response to CGRP in HSCs. Cells were preincubated with DIPMA-MK-3207 or MK-3207 (1-1000 nM) for 20 min at room temperature to allow nanoparticle accumulation in endosomes. Cells were washed, challenged with CGRP (1 µM), and Ca2+ responses were measured for 40 min. Maximal responses are shown. (i, j) PMA in C57BL/6J mice. Mice were pretreated by periorbital injection of DIPMA-MK-3207, MK-3207 (0.1, 0.3, 1 pmol), DIPMA-Ø or vehicle. After 30 min, mice received periorbital injections of CGRP (1.5 nmol) (l), capsaicin (CPS, 50 pmol) (j) or vehicle. (n=8 mice per group). Mean±SEM. ***P<0.001 vs. DIPMA-Ø/Veh, ##P<0.01, ###P<0.001 vs. MK-3207 0.3 pmol and MK-3207 1 pmol. (f) 2-way ANOVA, Bonferroni correction.

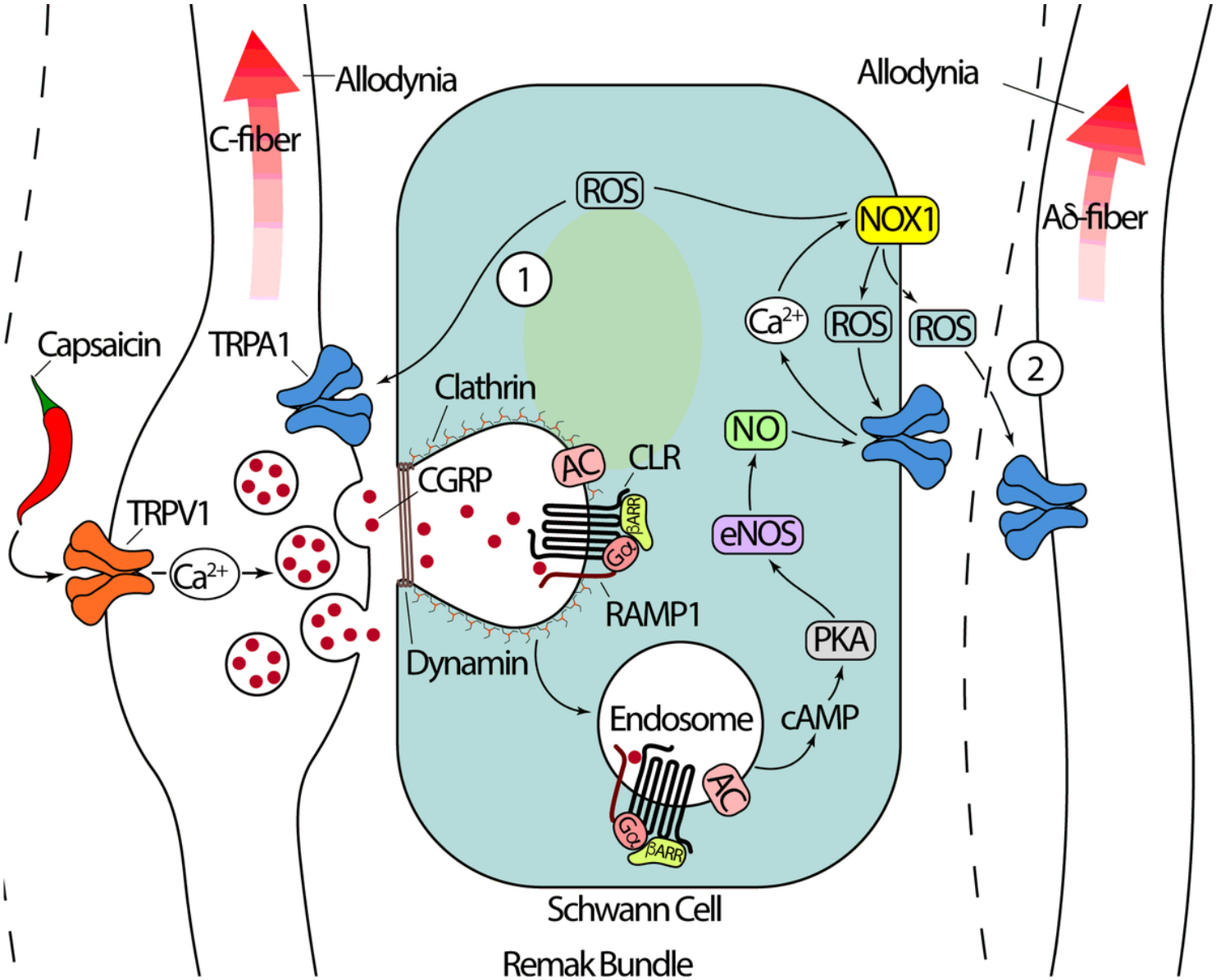

Figure 9

Schematic representation of the pathway that signal prolonged cutaneous allodynia elicited by CGRP released and associated with neurogenic inflammation. The pro-migraine neuropeptide, CGRP, released from trigeminal cutaneous afferents, activates CLR/RAMP1 on Schwann cells. CLR/RAMP1 traffics to endosomes, where sustained G protein signaling increases cAMP and stimulates PKA that results in nitric oxide synthase activation. The ensuing release of nitric oxide targets the oxidant-sensitive channel, TRPA1, in Schwann cells, which elicits persistent ROS generation. ROS triggers TRPA1 on adjacent C- (1) or Aδ-fiber (2) afferents resulting in periorbital allodynia, a hallmark of migraine pain.

Supplementary Files

This is a list of supplementary files associated with this preprint. Click to download.

- DeLoguSupplMaterial.pdf
- SuppVideo1.mp4
- SuppVideo2.mp4
- SuppVideo3.mp4
- SuppVideo4.mp4
- SuppVideo5.mp4
- SuppVideo6.mp4
- NCOMMS2128409nrreportingsummary3.pdf